

JET PROPULSION LABORATORY

SIRTF IPF REPORT

JPL ID103087

October 27, 2003

**SIRTF INSTRUMENT POINTING FRAME  
KALMAN FILTER EXECUTION SUMMARY**

IPF RUN NUMBER: 103087

REPORT TYPE: IOC EXECUTION (COARSE)

PRIME FRAME: MIPS\_160um\_center\_large\_FOV (87)

INFERRRED FRAMES: (88) (89) (91) (92)

**IPF TEAM**

Autonomy and Control Section (345)

Jet Propulsion Laboratory

California Institute of Technology

4800 Oak Grove Drive

Pasadena, CA 91109

# Contents

<b>1 IPF EXECUTION SUMMARY</b>	<b>5</b>
<b>2 IPF INPUT FILE HISTORY</b>	<b>9</b>
<b>3 IPF EXECUTION RESULTS</b>	<b>12</b>
3.1 IPF EXECUTION OUTPUT PLOTS . . . . .	12
3.2 IPF OUTPUT DATA (IF MINI FILE) . . . . .	36
3.3 IPF EXECUTION LOG . . . . .	39
<b>4 COMMENTS</b>	<b>42</b>

## List of Figures

1.1 A-priori and a-posteriori IPF frames . . . . .	5
1.2 A-priori and a-posteriori IPF frames (ZOOMED) . . . . .	8
2.1 Scenario Plot . . . . .	9
2.2 Attitude file edit history . . . . .	10
2.3 Centroid file edit history . . . . .	10
2.4 Oriented PixelCoords of Centroid Meas. Edited Centroids . . . . .	11
3.1 TPF coords of measurements and a-priori predicts . . . . .	14
3.2 Oriented PixelCoords of measurements and a-priori predicts . . . . .	14
3.3 Oriented (W,V) PixelCoords of A-Priori Prediction Error Quiver Plot . . . . .	15
3.4 A-priori prediction error (Science Centroids) . . . . .	15
3.5 Oriented PixelCoords of measurements and a-priori predicts (PCRS only) . . . . .	16
3.6 Oriented PixelCoords of measurements and a-priori predicts (Zoomed, PCRS only) . . . . .	16
3.7 Oriented (W,V) PixelCoords of A-Priori PCRS Prediction Error Quiver Plot . . . . .	17
3.8 A-priori PCRS prediction error . . . . .	17
3.9 IPF execution convergence, chart 1 . . . . .	18
3.10 IPF execution convergence, chart 2 . . . . .	18
3.11 Parameter uncertainty convergence . . . . .	19
3.12 IPF parameter symbol table . . . . .	19
3.13 KF parameter error sigma plots . . . . .	20
3.14 LS parameter error sigma plot . . . . .	20

3.15	KF and LS parameter error sigma plot . . . . .	21
3.16	Oriented Pixel Coords of meas. and a-posteriori predicts . . . . .	22
3.17	Oriented Pixel Coords of meas. and a-posteriori predicts (attitude corrected) . . . . .	22
3.18	KF innovations with (o) and w/o (+) attitude corrections . . . . .	23
3.19	Histograms of science a-posteriori residuals (or innovations) . . . . .	23
3.20	KF innovations with (o) and w/o (+) attitude corrections (PCRS) . . . . .	24
3.21	Histograms of PCRS a-posteriori residuals (or innovations) . . . . .	24
3.22	A-Posteriori Science Centroid Prediction Error Quiver (Att. Cor.) . . . . .	25
3.23	Normalized A-Posteriori Science Centroid Prediction Errors . . . . .	25
3.24	A-Posteriori PCRS Prediction Errors Quiver (Att. Cor.) . . . . .	26
3.25	Normalized A-Posteriori PCRS Prediction Errors . . . . .	26
3.26	W-axis KF innovations and 1-sigma bound . . . . .	27
3.27	V-axis KF innovations and 1-sigma bound . . . . .	27
3.28	Array plot with (solid) and w/o (dashed) optical distortion corrections . . . . .	28
3.29	Optical Distortion Plot: total (x5 magnification) . . . . .	28
3.30	Optical Distortion Plot: constant plate scales (x5 magnification) . . . . .	29
3.31	Optical Distortion Plot: linear plate scale (x5 magnification) . . . . .	29
3.32	Optical Distortion Plot: gamma terms (x5 magnification) . . . . .	30
3.33	Scan Mirror Chops . . . . .	30
3.34	IPF Frame Reconstruction . . . . .	31
3.35	Center Pixel Reconstruction . . . . .	31
3.36	Estimated attitude corrections (Body frame) . . . . .	32
3.37	Estimated attitude error sigma plot (Body frame) . . . . .	32
3.38	Thermo-mechanical boresight drift (equiv. angle in (W,V) coords) . . . . .	33
3.39	Thermo-mechanical boresight drift (equiv. angle in Body frame) . . . . .	33
3.40	Gyro drift bias contribution (equiv. rate in (W,V) coords) . . . . .	34
3.41	Gyro drift bias contribution (equiv. angle in (W,V) coords) . . . . .	34
3.42	Gyro drift bias contribution (equiv. angle in Body frame) . . . . .	35

## List of Tables

1.1	IPF filter input files . . . . .	6
1.2	IPF filter execution configuration . . . . .	6

1.3	IPF filter execution mask vector assignment . . . . .	6
1.4	IPF calibration error summary ([arcsec], 1-sigma, radial) . . . . .	7
1.5	Measurement prediction error summary (1-sigma) . . . . .	7
1.6	IPF Brown angle summary . . . . .	8
2.1	IPF input file begin and end times . . . . .	9
2.2	IPF input file editing status . . . . .	9
2.3	List of Removed Centroids (Original CA File Row Index) . . . . .	11
3.1	Table of figures I (IPF run) . . . . .	12
3.2	Table of figures II (IPF run) . . . . .	13

# 1 IPF EXECUTION SUMMARY

This report summarizes the SIRTF Instrument Pointing Frame (IPF) Kalman Filter execution associated with run file: RN103087. In particular, this Focal Point Survey calibrates the instrument: MIPS\_160um\_center\_large\_FOV (87), as part of the IOC Coarse Survey. The main calibration results from the IPF filter execution have been documented in IF103087 typically stored in the mission archive DOM collection IPF\_IF. This report only summarizes the main aspects of the run, and does not substitute for the full information contained in the IF file.

Section 1 summarizes the filter execution results. The filter configurations are tabulated in Table 1.2 and the mask vector assignments are tabulated in Table 1.3. A total of 5 state parameters are estimated in this run. The overall End-to-End pointing performances are tabulated in Table 1.4. The prediction residuals throughout the estimation processes are tabulated in Table 1.5. Section 3 summarizes resulting plots, a mini summary of the IF IPF output file, and the execution log. Section 4 captures the user comments that are specific to this particular run.

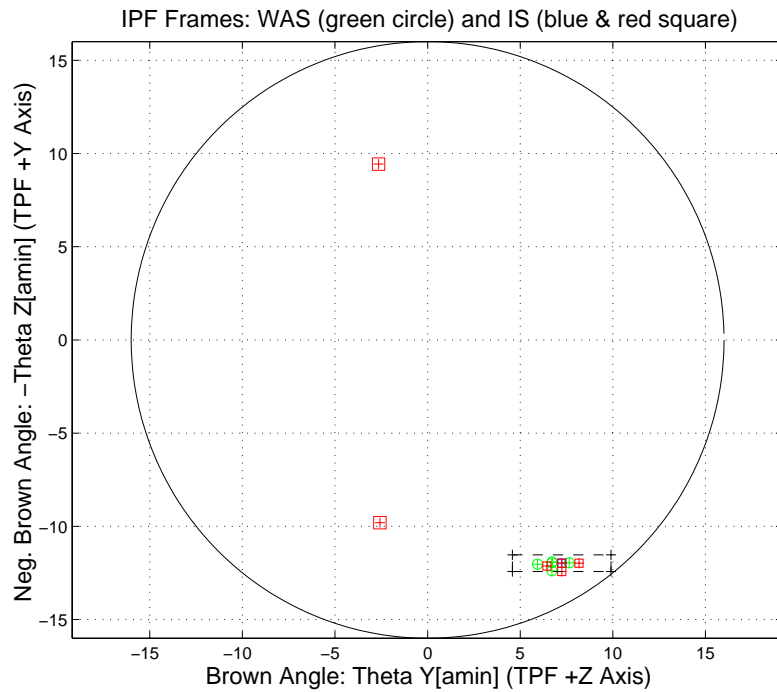


Figure 1.1: A-priori and a-posteriori IPF frames

RAW	FINAL (After Editing)
AA101087	AA101087
AS101087	AS101087
CA101087	CA191087
CB101087	CB101087
CS101087	CS102087

Table 1.1: IPF filter input files

EXECUTION CONFIGURATION ITEM	CURRENT STATUS
IPF Filter Version Used	IPF.V2.0.0D
Frame Table Version Used	BodyFrames_FTU_11a
Scan-Mirror Employed?	NO
IPF Filter Mode	LITE-MODE(3):FLT
SLIT-MODE Operation	DISABLED
Kalman Filter Operation	ENABLED
Least-Squares Data Analysis	ENABLED
IBAD Screening	ENABLED
User-Specified Data Editing	DISABLED
Total Number of Iterations	30
LS Residual Sigma Scale	2.48686089E+00
Total Number of Maneuvers	12

Table 1.2: IPF filter execution configuration

Con. Plate Scale			$\Gamma$ Dependent				$\Gamma^2$ Dependent				Linear Plate Scale						Mirror			
$a_{00}$	$b_{00}$	$c_{00}$	$a_{10}$	$b_{10}$	$c_{10}$	$d_{10}$	$a_{20}$	$b_{20}$	$c_{20}$	$d_{20}$	$a_{01}$	$b_{01}$	$c_{01}$	$d_{01}$	$e_{01}$	$f_{01}$	$\alpha$	$\beta$		
1	2	3	4	5	6	7	8	9	10	11	12	13	14	15	16	17	18	19		
0	0	0	0	0	0	0	0	0	0	0	0	0	0	0	0	0	0	0		
IPF (T)			Alignment R						Gyro Drift Bias											
$\theta_1$	$\theta_2$	$\theta_3$	$a_{rx}$	$a_{ry}$	$a_{rz}$	$b_{rx}$	$b_{ry}$	$b_{rz}$	$c_{rx}$	$c_{ry}$	$c_{rz}$	$b_{gx}$	$b_{gy}$	$b_{gz}$	$c_{gx}$	$c_{gy}$	$c_{gz}$			
20	21	22	23	24	25	26	27	28	29	30	31	32	33	34	35	36	37			
0	1	1	1	1	1	0	0	0	0	0	0	0	0	0	0	0	0			

Table 1.3: IPF filter execution mask vector assignment

## FOCAL PLANE SURVEY ANALYSIS: IOC Coarse Survey.

INSTRUMENT NAME: MIPS\_160um\_center\_large\_FOV NF: 87

PIX2RADW: 7.73998982E-05 [rad/pixel] = 1.5965E+01 [arcsec/pixel]

PIX2RADV: 8.70861410E-05 [rad/pixel] = 1.7963E+01 [arcsec/pixel]

FRAME	DESCRIPTION	IPF <sup>1</sup>	SF <sup>2</sup>	TOTAL	REQ
087(P)	MIPS_160um_center_large_FOV	3.7849	0.0855	3.7858	3.75
088(I)	MIPS_160um_plusY_edge	3.7849	0.0855	3.7858	N/A
089(I)	MIPS_160um_large_only	3.7849	0.0855	3.7858	N/A
091(I)	MIPS_160um_small_FOV1	3.7849	0.0855	3.7858	N/A
092(I)	MIPS_160um_small_FOV2	3.7849	0.0855	3.7858	N/A

Table 1.4: IPF calibration error summary ([arcsec], 1-sigma, radial)

RMS METRIC	A PRIORI <sup>3</sup>	A POSTERIORI <sup>3</sup>	ATT. CORRECTED <sup>4</sup>	UNITS
Radial	15.0021	6.8989	6.9000	arcsec
W-Axis	14.7380	4.4895	4.4990	arcsec
V-Axis	2.8027	5.2383	5.2316	arcsec
Radial	0.9362	0.4051	0.4053	pixels
W-Axis	0.9232	0.2812	0.2818	pixels
V-Axis	0.1560	0.2916	0.2912	pixels

Table 1.5: Measurement prediction error summary (1-sigma)

---

<sup>1</sup>IPF filter removes systematic pointing errors due to: thermomechanical alignment drift (Body to TPF), gyro bias and bias drift, centroiding error, attitude error, and optical distortion. IPF SIGMA presented here is “Scaled” by the Least Squares Scale factor. The Least Squares Scale Factor was: 2.486861. It is assumed that the gyro Angle Random Walk contribution is captured with the Least Squares scaling. The gyro ARW contribution can be approximately calculated as 0.0600 arcseconds, given that ARW = 100  $\mu\text{deg}/\sqrt{\text{hr}}$ , with 5.992395e+02 second Maneuver time (max), and 12 independent Maneuvres.

<sup>2</sup>Gyro Scale Factor(GSF) assumes 95 ppm error over 0.250 degree maneuver.

<sup>3</sup>This can be interpreted as estimate of ”pixel to sky” pointing reconstruction error if no science data is used.

<sup>4</sup>This can be interpreted as estimate of achieved S/I centroiding error

IPF BROWN ANGLE SUMMARY					
FRAME TABLE USED: BodyFrames_FTU_11a					
NF	NAME	WAS	IS	CHANGE	UNIT
087	theta_Y	+6.720661	+7.240265	+0.519605	arcmin
087	theta_Z	+11.925107	+11.975320	+0.050214	arcmin
087	angle	+0.000000	+0.000002	+0.000002	deg
088	theta_Y	+6.715660	+7.240265	+0.524605	arcmin
088	theta_Z	+12.382106	+12.424391	+0.042285	arcmin
088	angle	-0.000000	+0.000002	+0.000002	deg
089	theta_Y	+6.720661	+7.240265	+0.519605	arcmin
089	theta_Z	+11.925107	+11.975320	+0.050214	arcmin
089	angle	+0.000000	+0.000002	+0.000002	deg
091	theta_Y	+7.640661	+8.171550	+0.530889	arcmin
091	theta_Z	+11.954106	+11.975320	+0.021214	arcmin
091	angle	+0.000000	+0.000002	+0.000002	deg
092	theta_Y	+5.930660	+6.442022	+0.511361	arcmin
092	theta_Z	+12.034106	+12.125011	+0.090904	arcmin
092	angle	-0.000000	+0.000002	+0.000002	deg

Table 1.6: IPF Brown angle summary

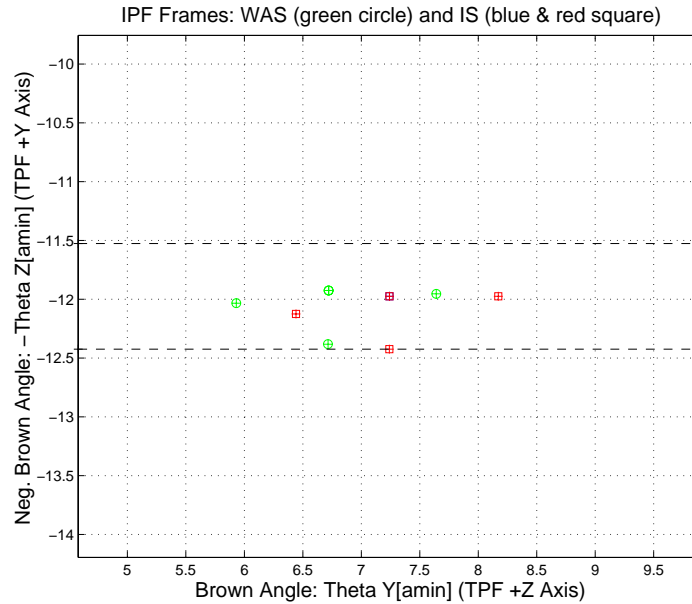


Figure 1.2: A-priori and a-posteriori IPF frames (ZOOMED)

## 2 IPF INPUT FILE HISTORY

STATUS	FILENAME	START TIME	END TIME
WAS	AA101087	751560000.3	751569000.2
IS	AA101087	751560000.3	751569000.2
WAS	CA101087	751560823.5	751565422.5
IS	CA191087	751560823.5	751565422.5
WAS	CB101087	751560667.4	751568163.4
IS	CB101087	751560667.4	751568163.4

Table 2.1: IPF input file begin and end times

WAS	SIZE	IS	SIZE	REMOVED	PATCHED
AA101087	90000	AA101087	90000	0	0
CA101087	23	CA191087	20	3	N/A
CB101087	72	CB101087	72	0	N/A

Table 2.2: IPF input file editing status

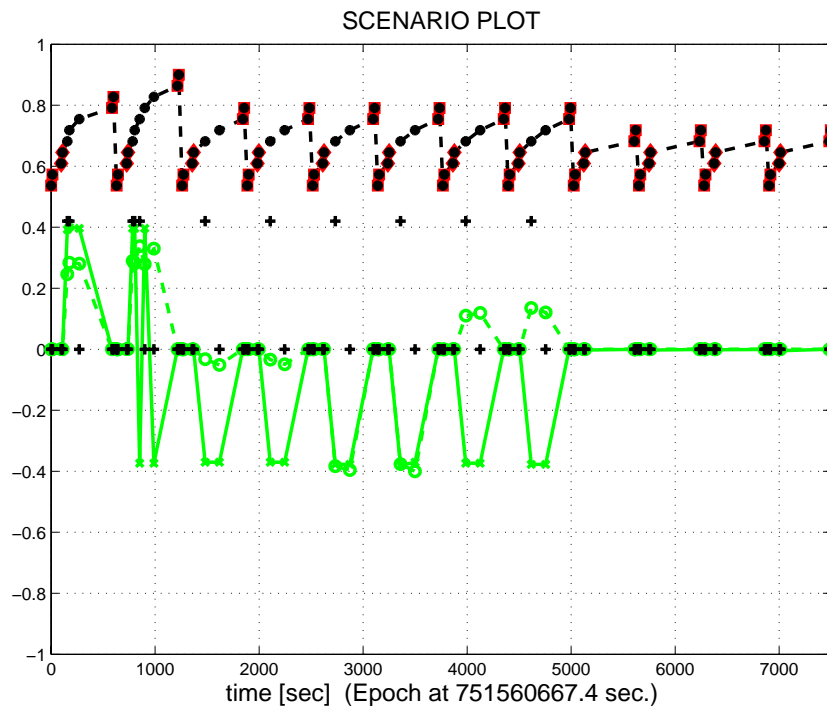


Figure 2.1: Scenario Plot

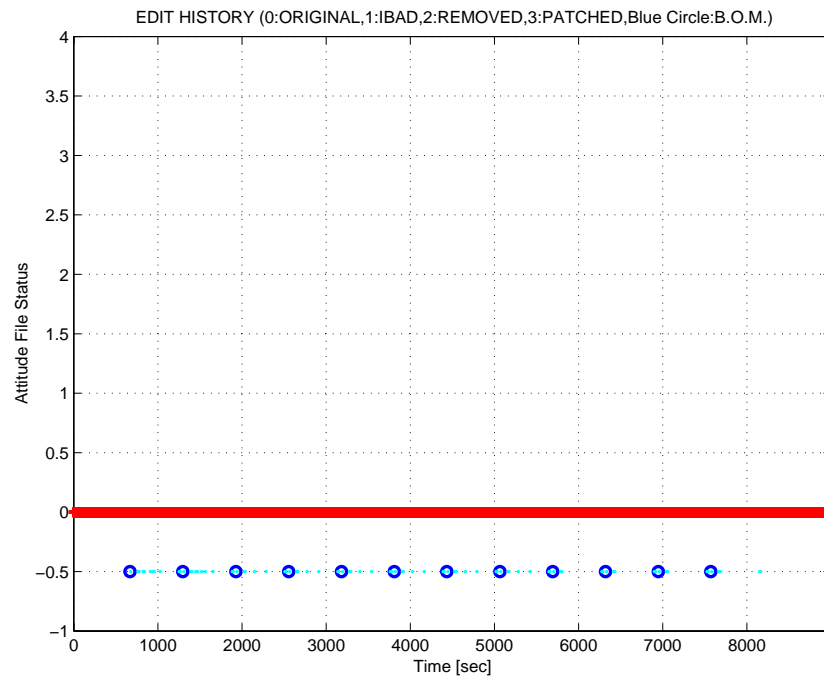


Figure 2.2: Attitude file edit history

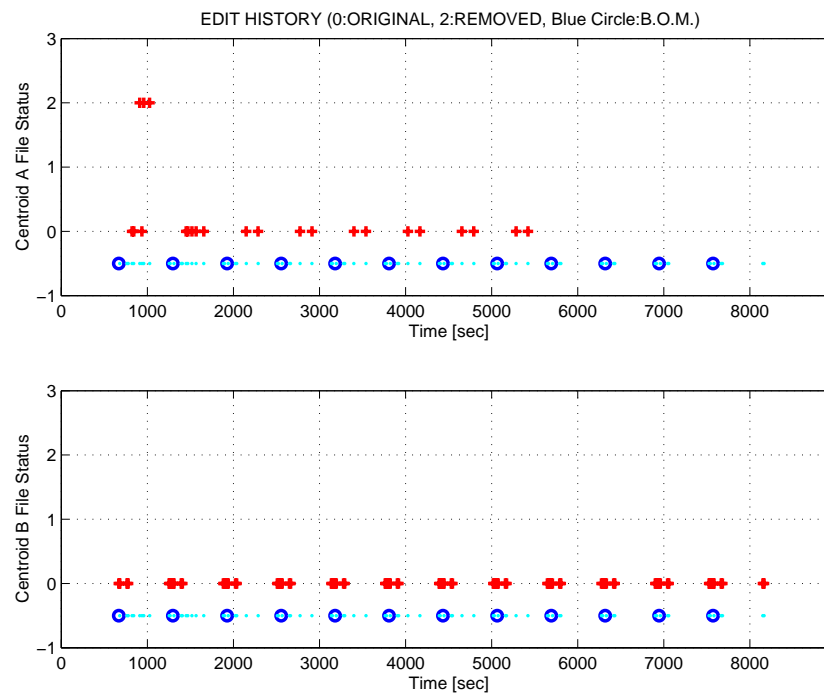


Figure 2.3: Centroid file edit history

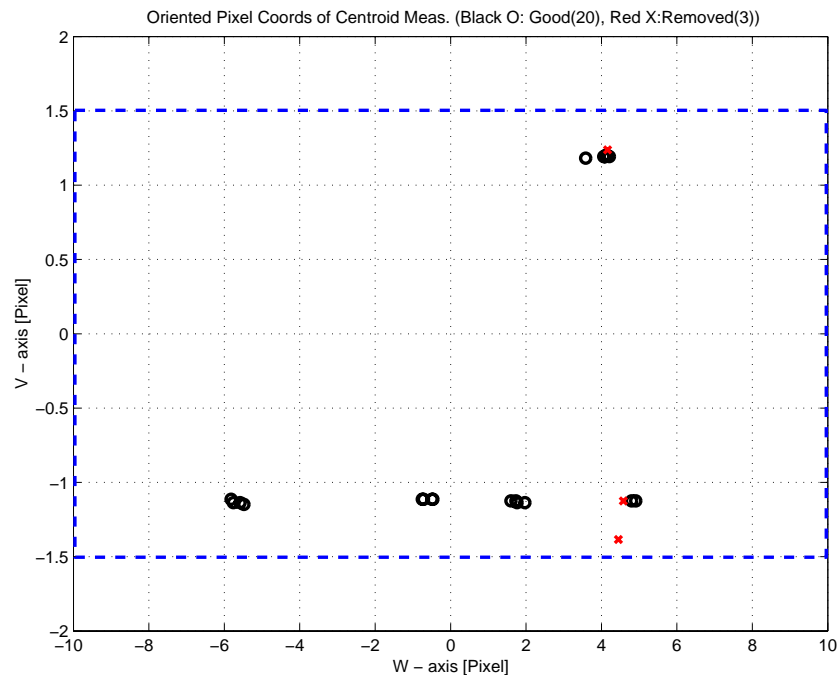


Figure 2.4: Oriented Pixel Coords of Centroid Meas. Edited Centroids

LIST OF REMOVED CENTROIDS										
1	2	3	4	5	6	7	8	9	10	
3	5	6								

Table 2.3: List of Removed Centroids (Original CA File Row Index)

### 3 IPF EXECUTION RESULTS

#### 3.1 IPF EXECUTION OUTPUT PLOTS

This subsection summarizes the IPF filter results. As shown in Table 3.1, the output plots are segmented to three groups: predicted performance, post-run results and IPF trending plots.

FIGURE NO.	DESCRIPTION
<b>Predicted performance prior to IPF run</b>	
Figure 3.1	Meas. and a-priori predicts in TPF coords
Figure 3.2	Meas. and a-priori predicts in Oriented Pixel Coords including rectangular array boundary approximation
Figure 3.3	A-Priori Prediction Error Quiver Plot in Oriented Pixel Coords including rectangular array boundary approximation
Figure 3.4	A-priori prediction error
Figure 3.5	Oriented Pixel Coords of measurements and a-priori predicts (PCRS only)
Figure 3.6	Oriented Pixel Coords of measurements and a-priori predicts (Zoomed, PCRS only)
Figure 3.7	Oriented (W,V) Pixel Coords of A-Priori PCRS Prediction Error Quiver Plot
Figure 3.8	A-priori PCRS prediction error
<b>IPF filter performance (post run results)</b>	
Figure 3.9	IPF execution convergence, chart 1: (top) normalized residual error vs. iteration number and (bottom) norm of effective parameter corrections
Figure 3.10	IPF execution convergence, chart 2: parameter correction size vs. iteration number
Figure 3.11	Parameter uncertainty convergence: square-root of diagonal elements of covariance matrix vs. maneuver number
Figure 3.12	IPF parameter symbol table
Figure 3.13	KF parameter error sigma plot (a-priori-dashed, a-posteriori-solid). Includes true parameter errors (FLUTE runs only)
Figure 3.14	LS parameter error sigma plot. Includes true parameter errors (FLUTE runs only)
Figure 3.15	KF and LS parameter errors sigma plot (Figure 3.13 & Figure 3.14 combined)
Figure 3.16	Measurements and a-posteriori predicts in Oriented Pixel Coords including rectangular array boundaries (a-priori-dashed, a-posteriori-solid)
Figure 3.17	Attitude corrected meas. and a-posteriori predicts in Oriented Pixel Coords including rectangular array boundaries (a-priori-dashed, a-posteriori-solid)

Table 3.1: Table of figures I (IPF run)

FIGURE NO.	DESCRIPTION
<b>IPF filter performance (post run results) - CONTINUE</b>	
Figure 3.18	KF innovations with (o) and w/o (+) attitude corrections
Figure 3.19	Histograms of science a-posteriori residuals (or innovations)
Figure 3.20	KF innovations with (o) and w/o (+) attitude corrections (PCRS)
Figure 3.21	Histograms of PCRS a-posteriori residuals (or innovations)
Figure 3.22	A-Posteriori Science Centroid Prediction Error Quiver (Att. Cor.)
Figure 3.23	Normalized A-Posteriori Science Centroid Prediction Errors
Figure 3.24	A-Posteriori PCRS Prediction Errors Quiver (Att. Cor.)
Figure 3.25	Normalized A-Posteriori PCRS Prediction Errors
Figure 3.26	W-axis KF innovations and 1-sigma bound
Figure 3.27	V-axis KF innovations and 1-sigma bound
Figure 3.28	Array plot with (solid) and w/o (dashed) optical distortion corrections
Figure 3.29	Optical Distortion Plot: total (x5 magnification)
Figure 3.30	Optical Distortion Plot: constant plate scales (x5 magnification)
Figure 3.31	Optical Distortion Plot: linear plate scale (x5 magnification)
Figure 3.32	Optical Distortion Plot: gamma terms (x5 magnification)
Figure 3.33	Scan Mirror Chops
Figure 3.34	IPF Frame Reconstruction
Figure 3.35	Center Pixel Reconstruction
<b>IPF parameter trending plots</b>	
Figure 3.36	Estimated attitude corrections (Body frame)
Figure 3.37	Estimated attitude error sigma plot (Body frame)
Figure 3.38	Systematic error attributed to thermo-mechanical boresight drift (equiv. angle in (W,V) coords)
Figure 3.39	Systematic error attributed to thermo-mechanical boresight drift (equiv. angle in Body frame)
Figure 3.40	Systematic error attributed to gyro drift bias (equiv. rate in (W,V) coords)
Figure 3.41	Systematic error attributed to gyro drift bias (equiv. angle in (W,V) coords)
Figure 3.42	Systematic error attributed to gyro drift bias (equiv. angle in Body frame)

Table 3.2: Table of figures II (IPF run)

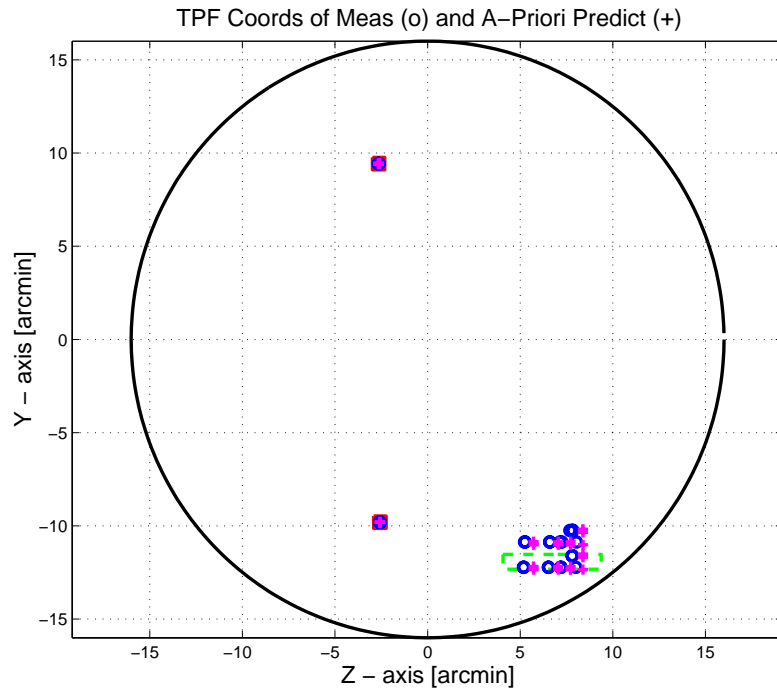


Figure 3.1: TPF coords of measurements and a-priori predicts

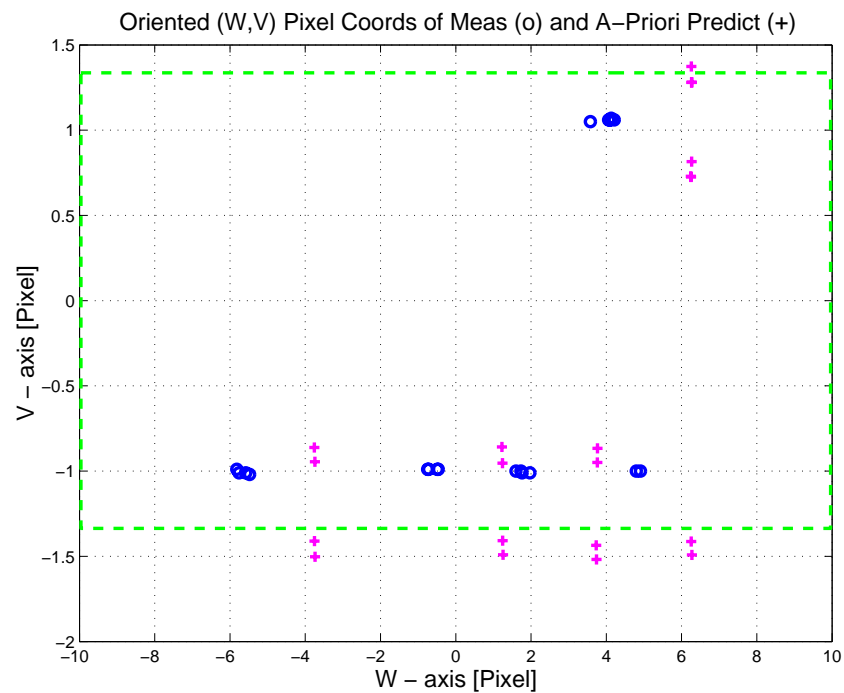


Figure 3.2: Oriented PixelCoords of measurements and a-priori predicts

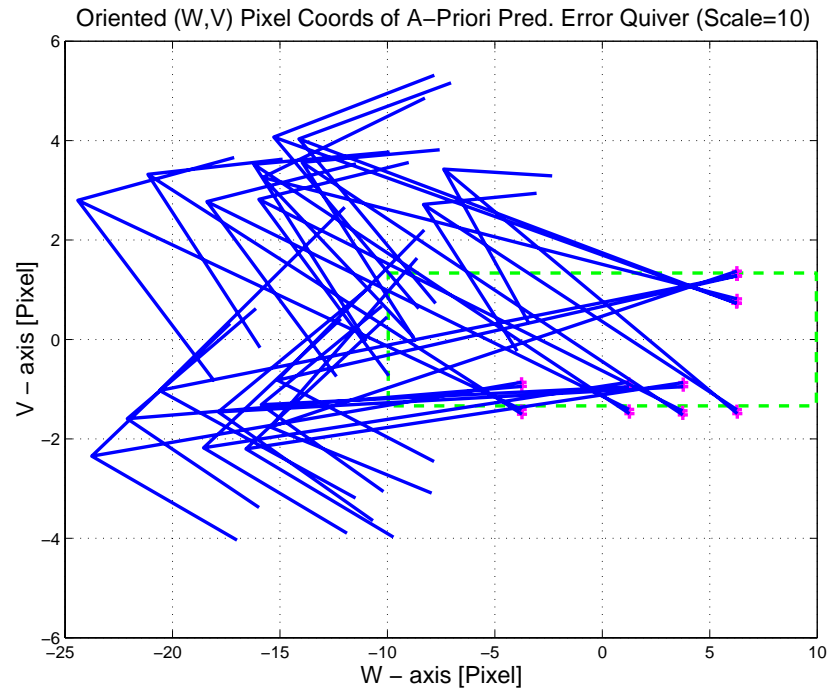


Figure 3.3: Oriented (W,V) Pixel Coords of A-Priori Prediction Error Quiver Plot

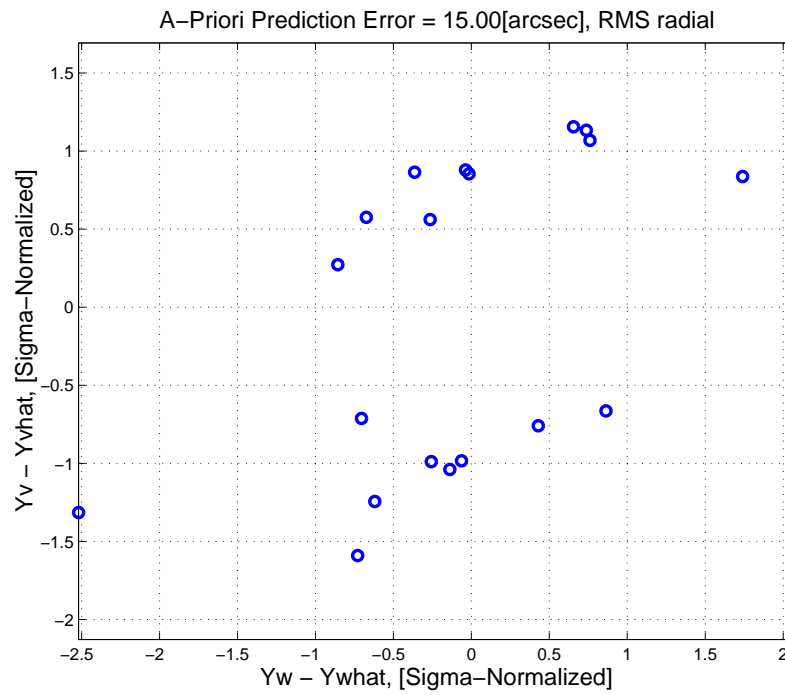


Figure 3.4: A-priori prediction error (Science Centroids)

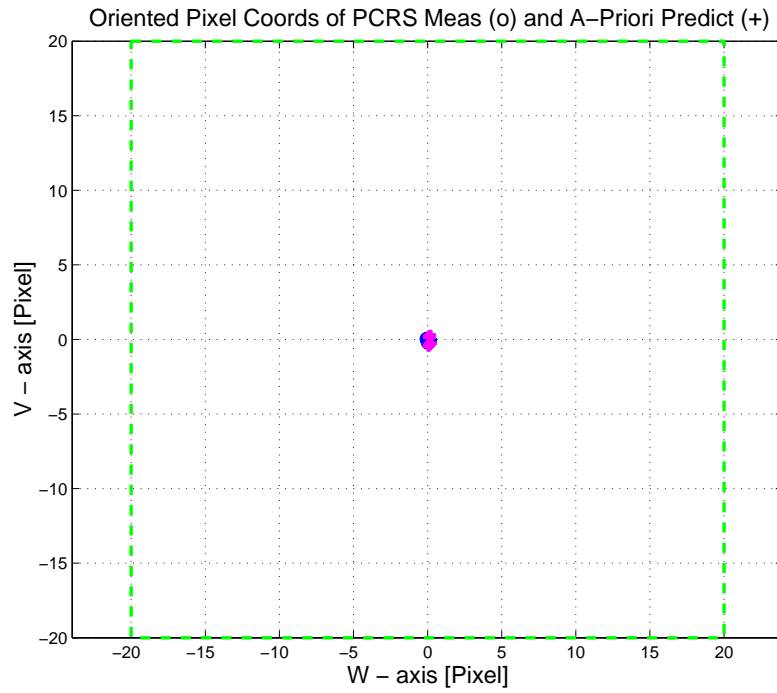


Figure 3.5: Oriented Pixel Coords of measurements and a-priori predicts (PCRS only)

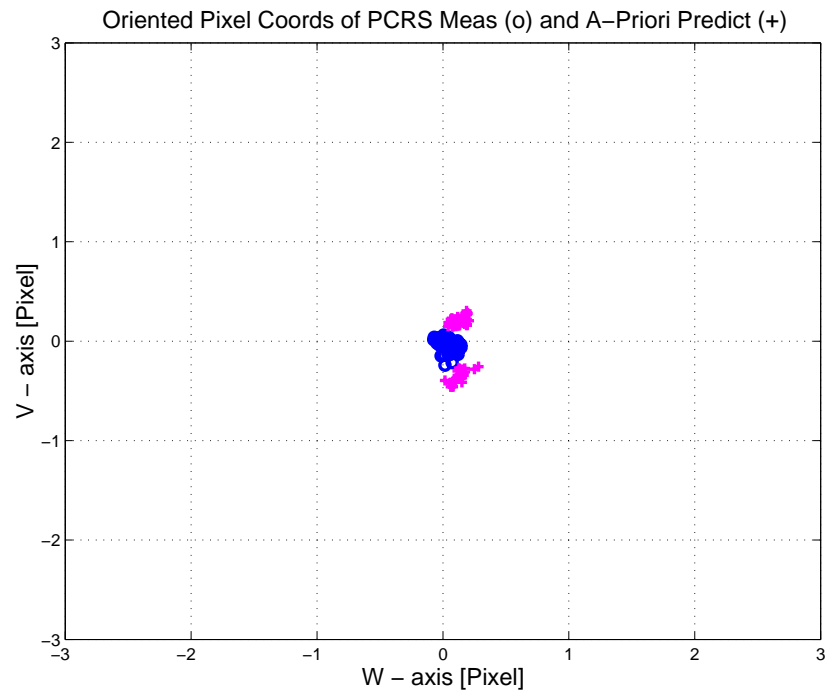


Figure 3.6: Oriented Pixel Coords of measurements and a-priori predicts (Zoomed, PCRS only)

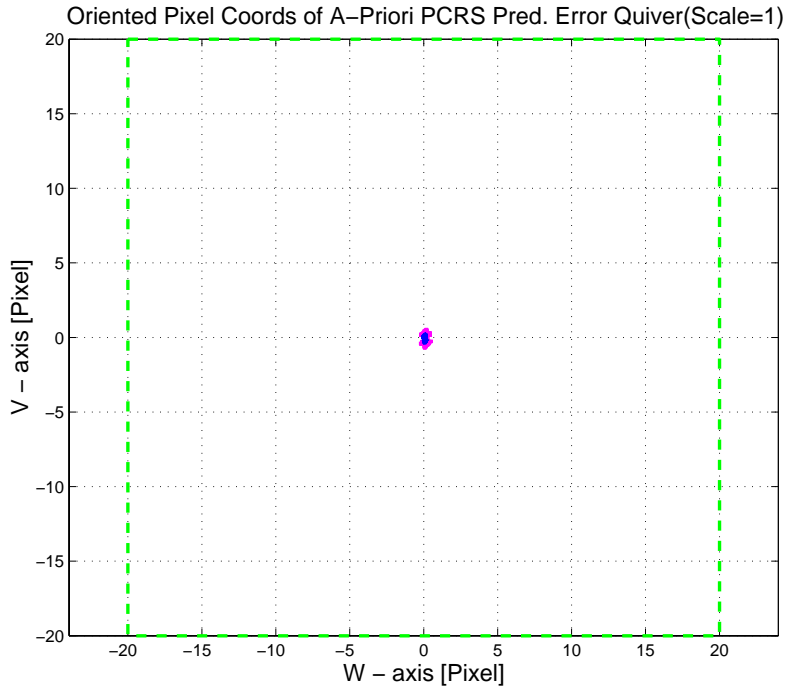


Figure 3.7: Oriented (W,V) Pixel Coords of A-Priori PCRS Prediction Error Quiver Plot

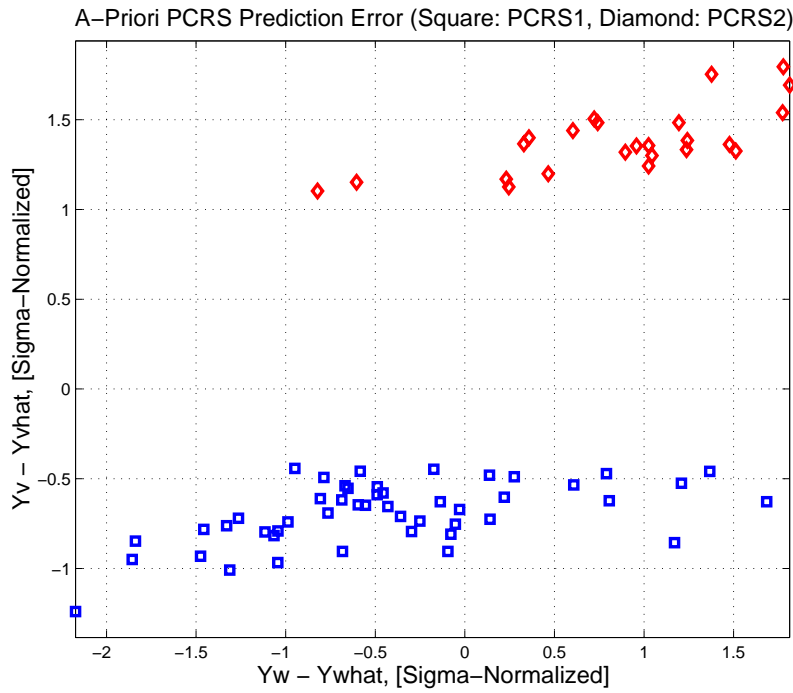


Figure 3.8: A-priori PCRS prediction error

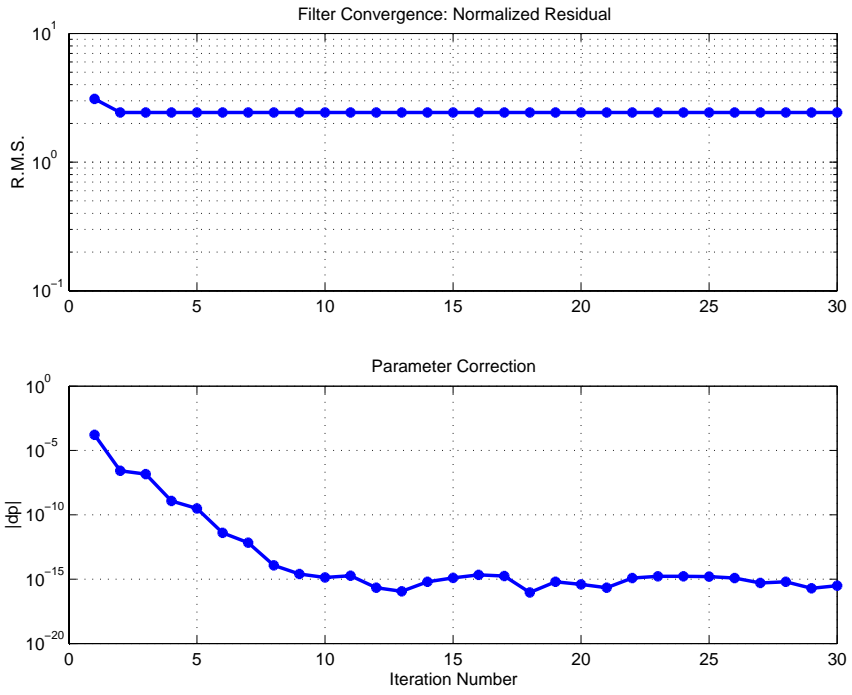


Figure 3.9: IPF execution convergence, chart 1

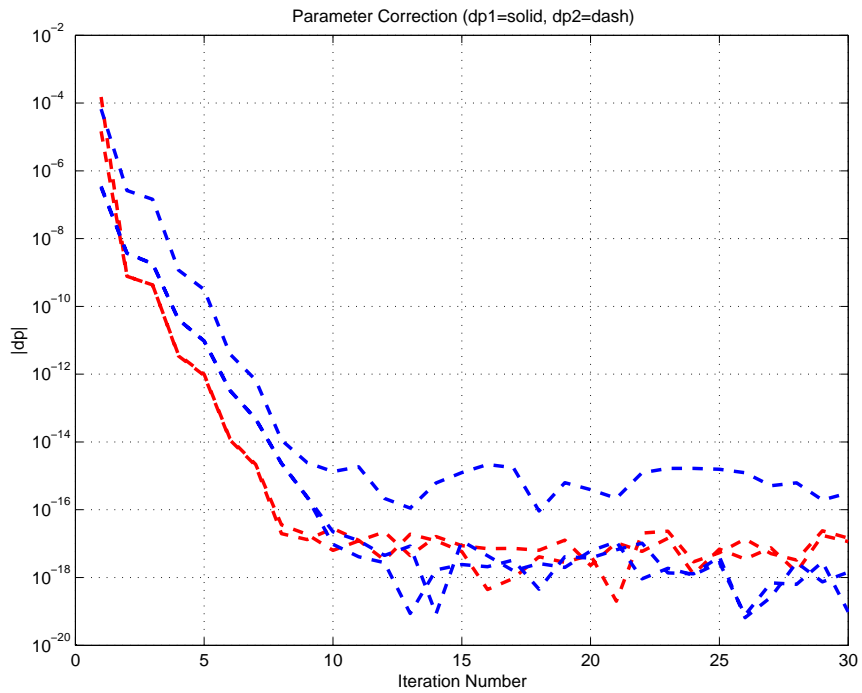


Figure 3.10: IPF execution convergence, chart 2

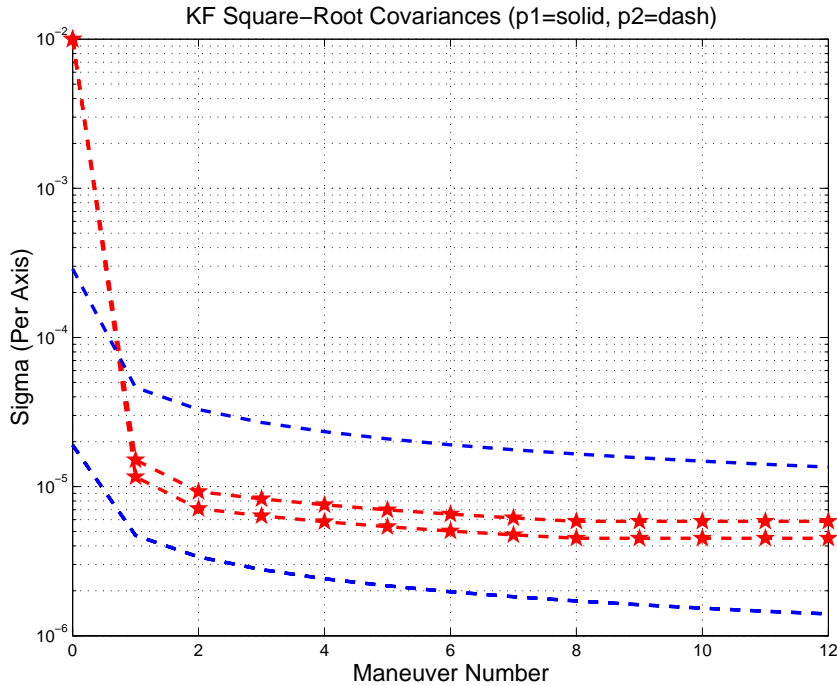


Figure 3.11: Parameter uncertainty convergence

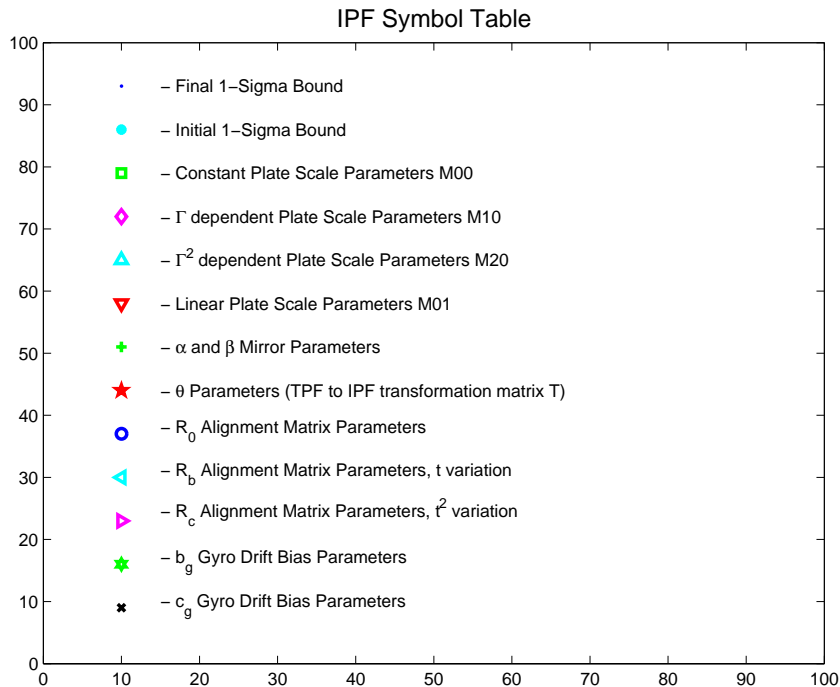


Figure 3.12: IPF parameter symbol table

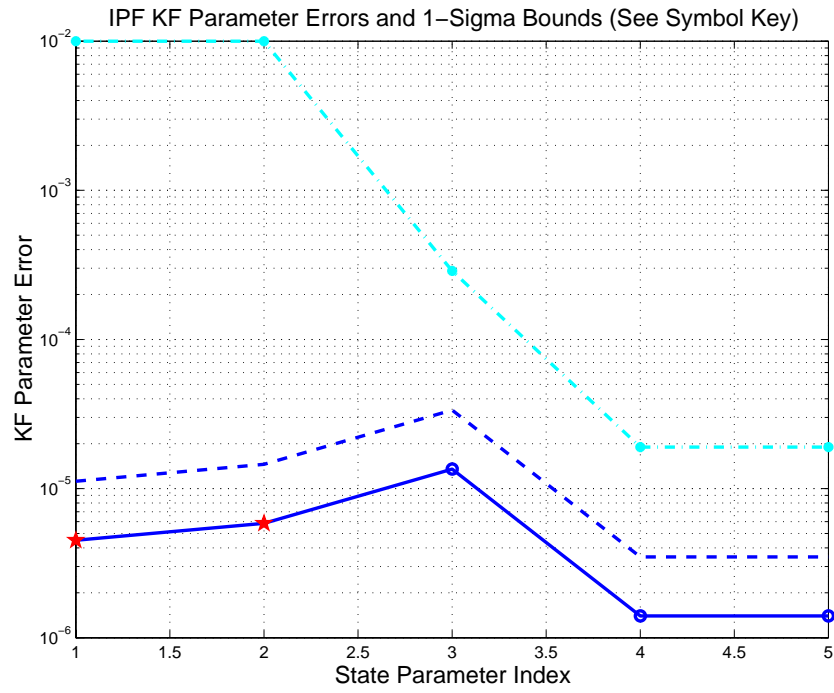


Figure 3.13: KF parameter error sigma plots

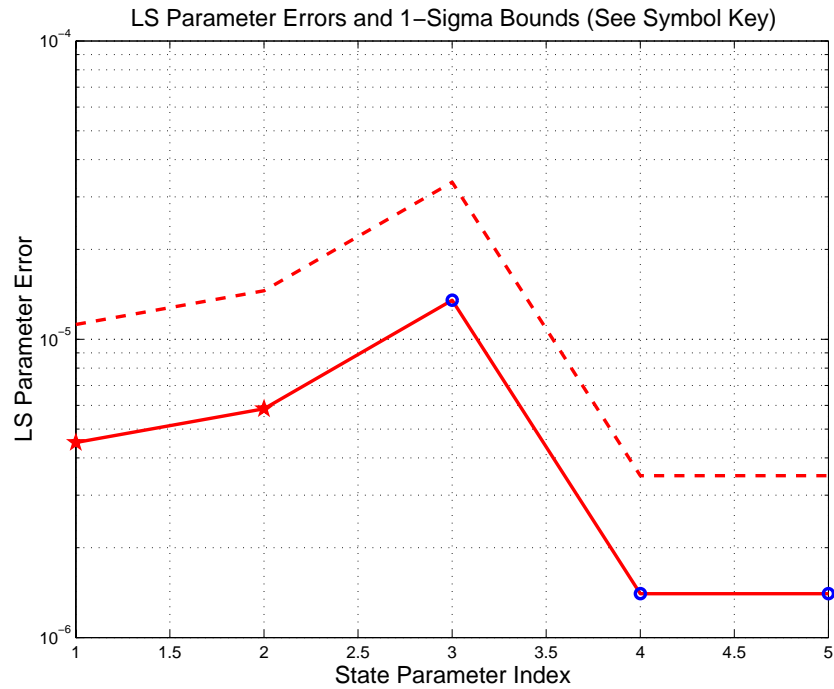


Figure 3.14: LS parameter error sigma plot

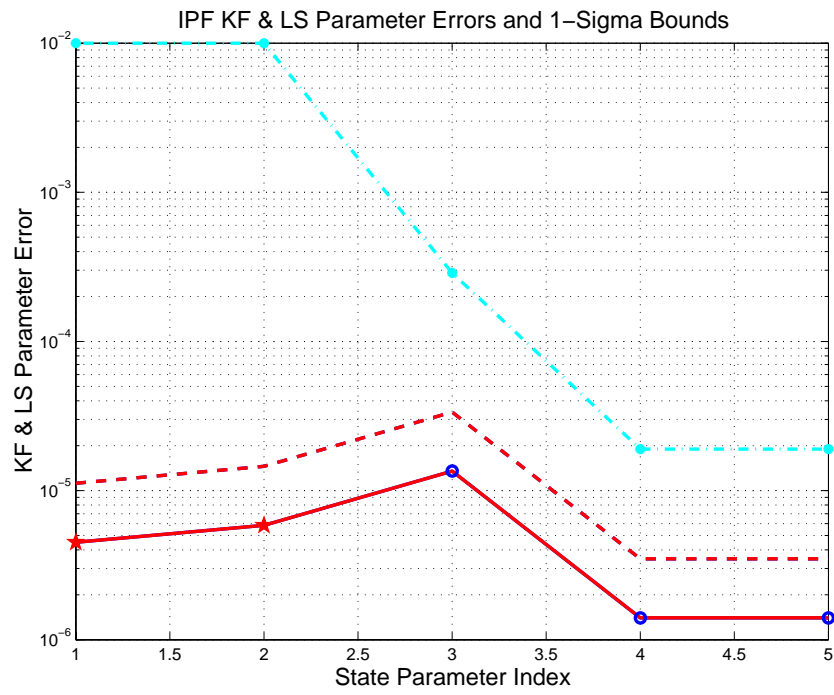


Figure 3.15: KF and LS parameter error sigma plot

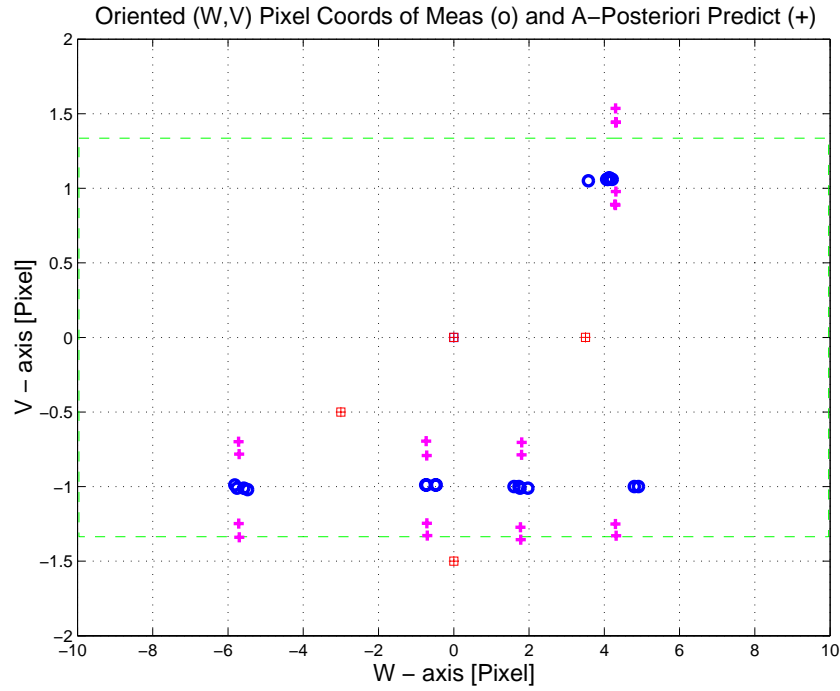


Figure 3.16: Oriented Pixel Coords of meas. and a-posteriori predicts

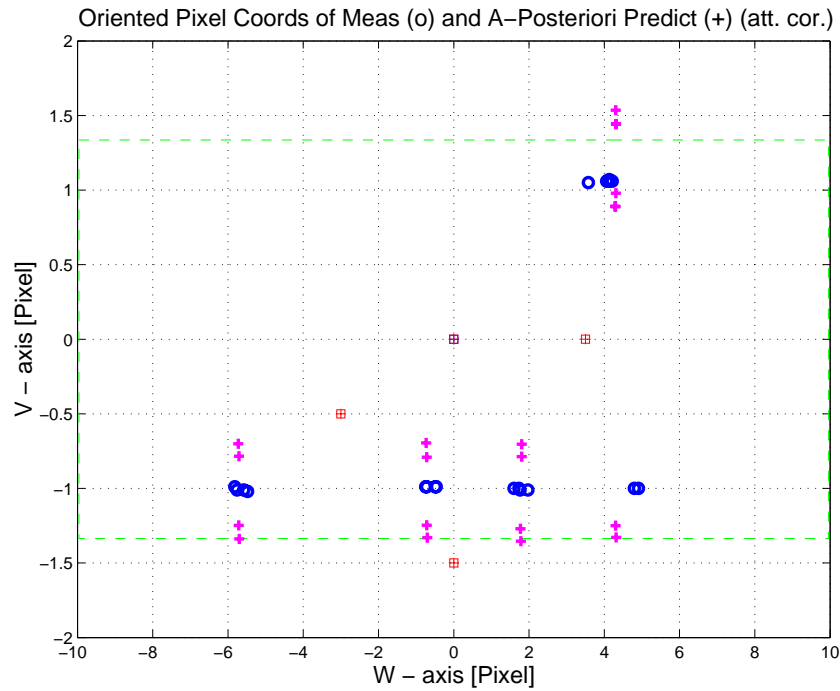


Figure 3.17: Oriented Pixel Coords of meas. and a-posteriori predicts (attitude corrected)

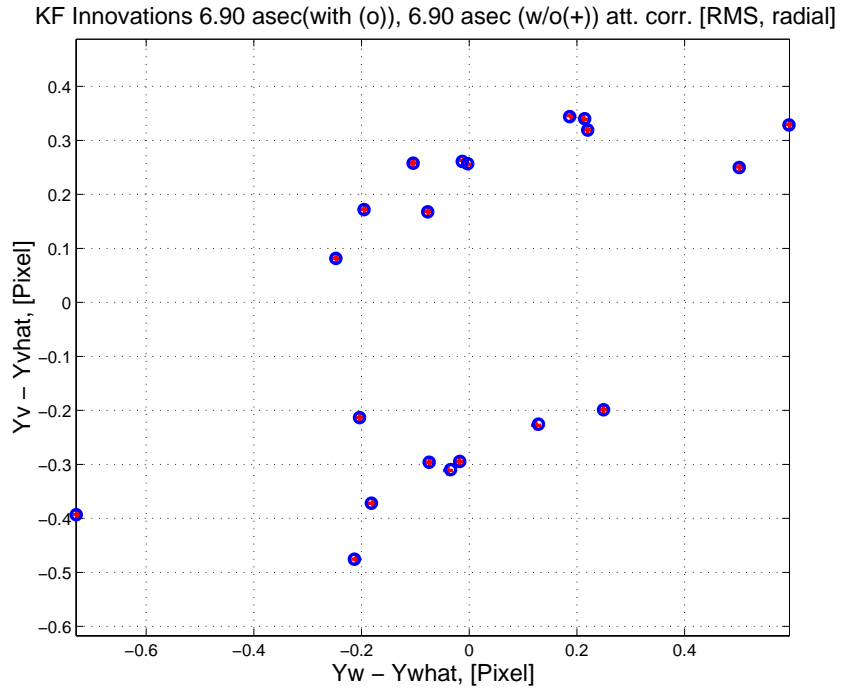


Figure 3.18: KF innovations with (o) and w/o (+) attitude corrections

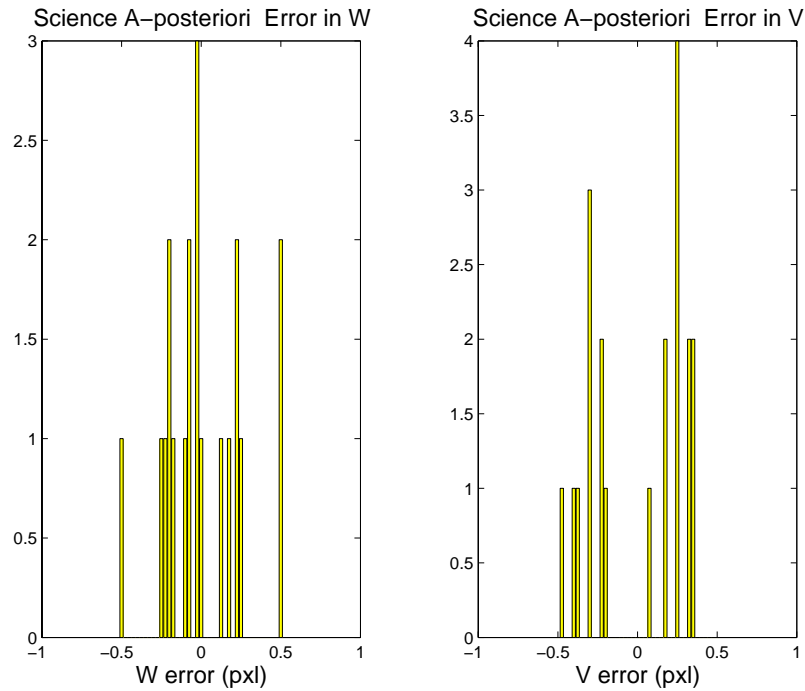


Figure 3.19: Histograms of science a-posteriori residuals (or innovations)

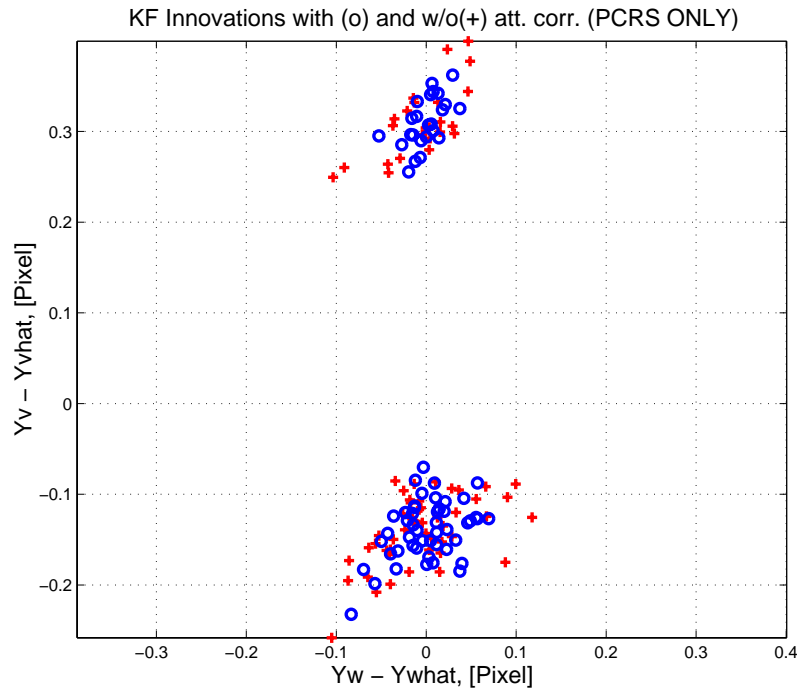


Figure 3.20: KF innovations with (o) and w/o (+) attitude corrections (PCRS)

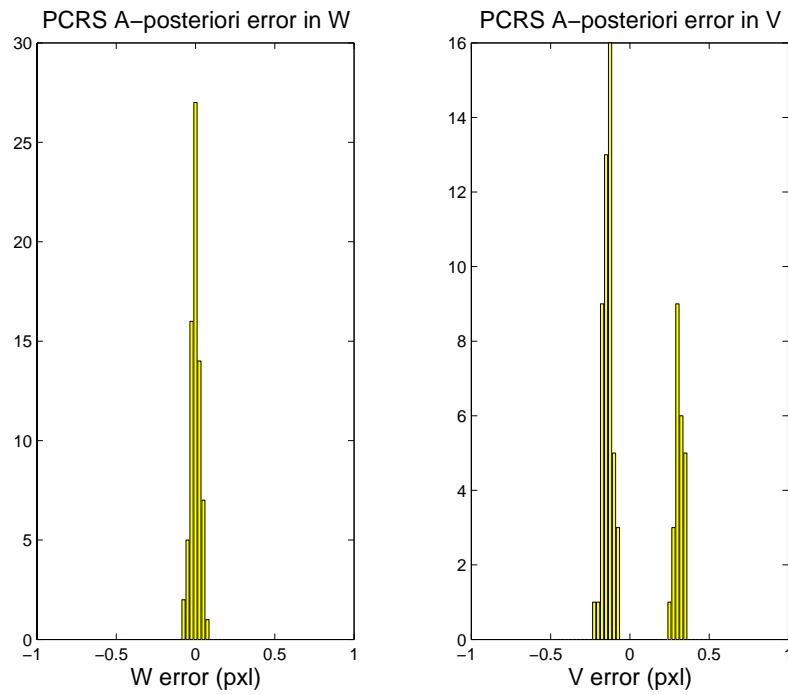


Figure 3.21: Histograms of PCRS a-posteriori residuals (or innovations)

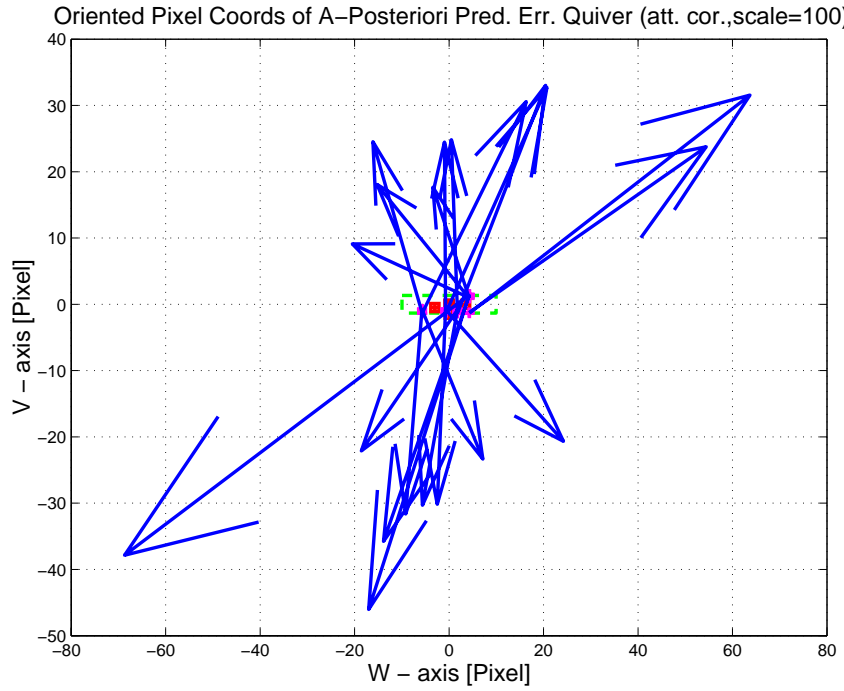


Figure 3.22: A-Posteriori Science Centroid Prediction Error Quiver (Att. Cor.)

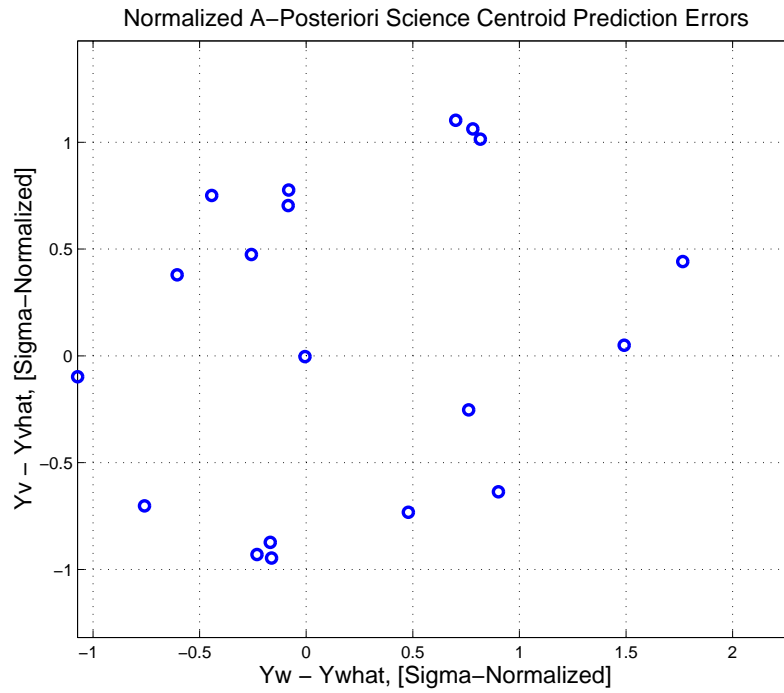


Figure 3.23: Normalized A-Posteriori Science Centroid Prediction Errors

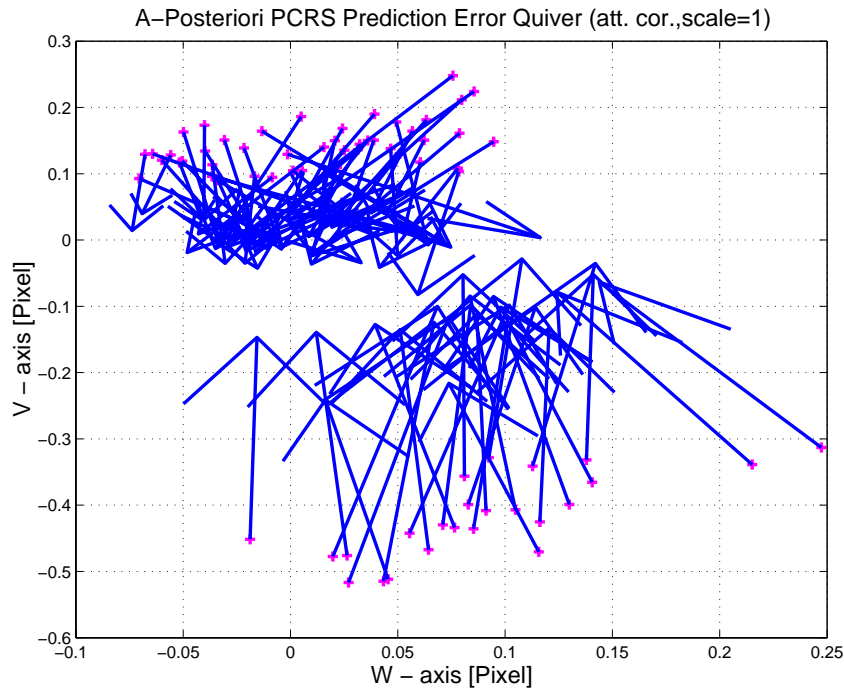


Figure 3.24: A–Posteriori PCRS Prediction Errors Quiver (Att. Cor.)

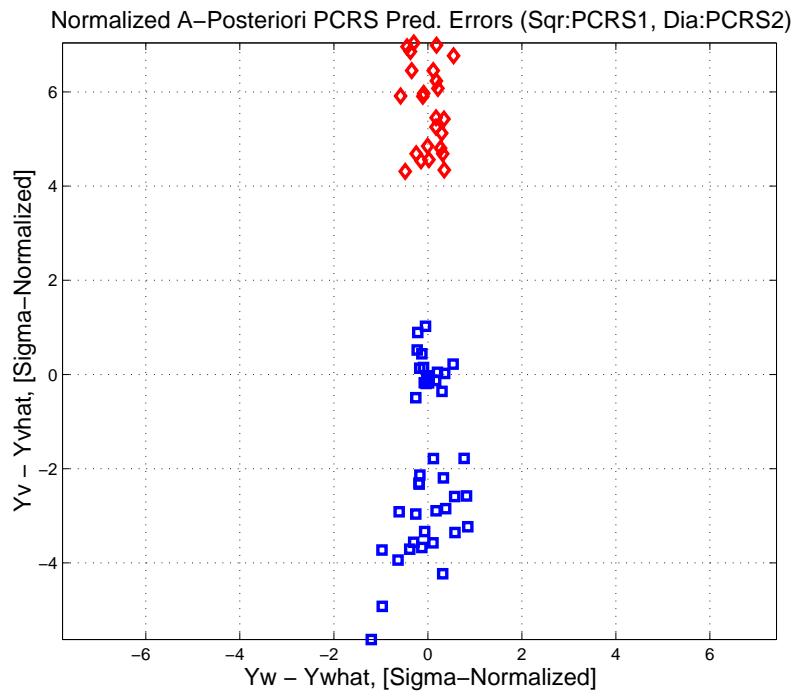


Figure 3.25: Normalized A–Posteriori PCRS Prediction Errors

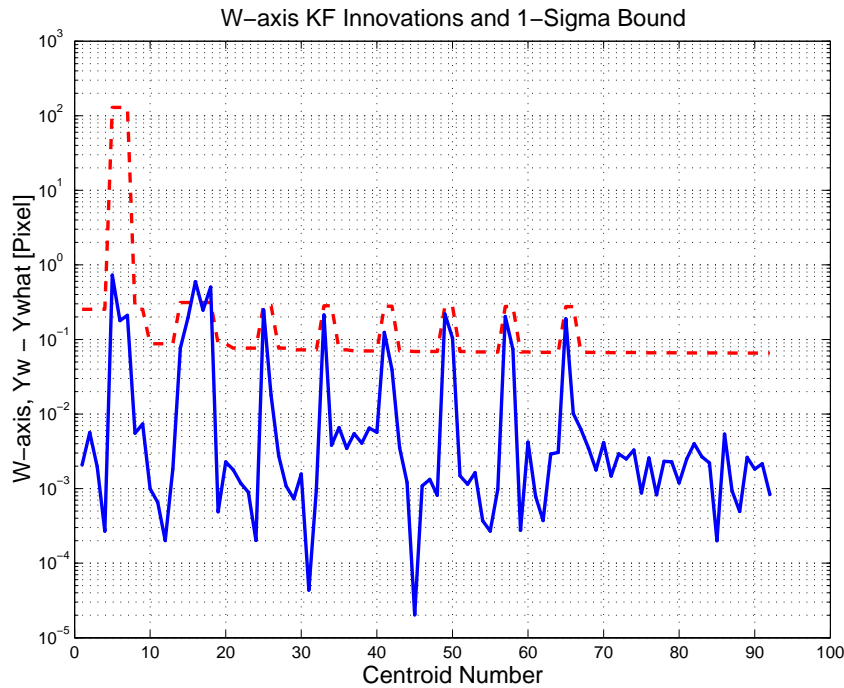


Figure 3.26: W-axis KF innovations and 1-sigma bound

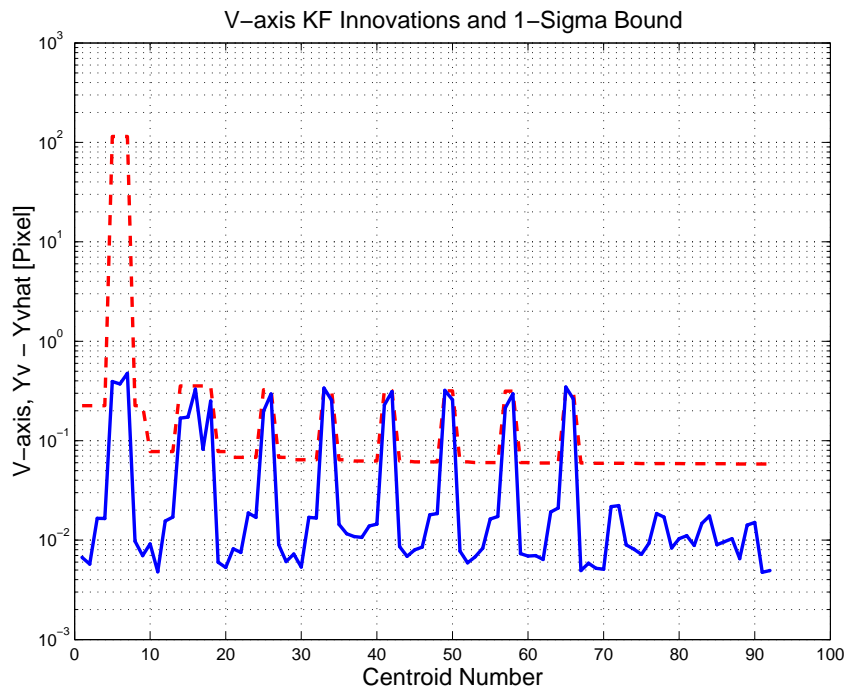


Figure 3.27: V-axis KF innovations and 1-sigma bound

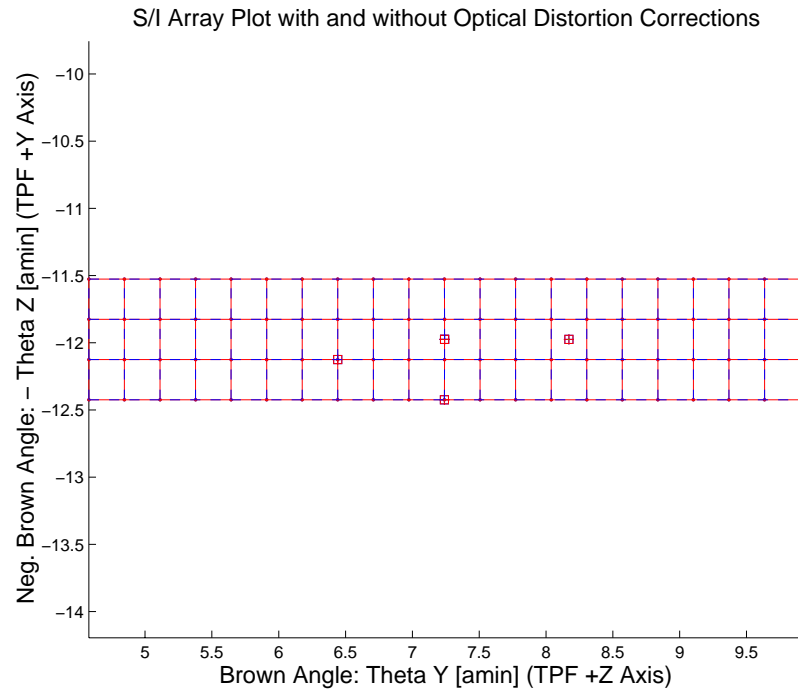


Figure 3.28: Array plot with (solid) and w/o (dashed) optical distortion corrections

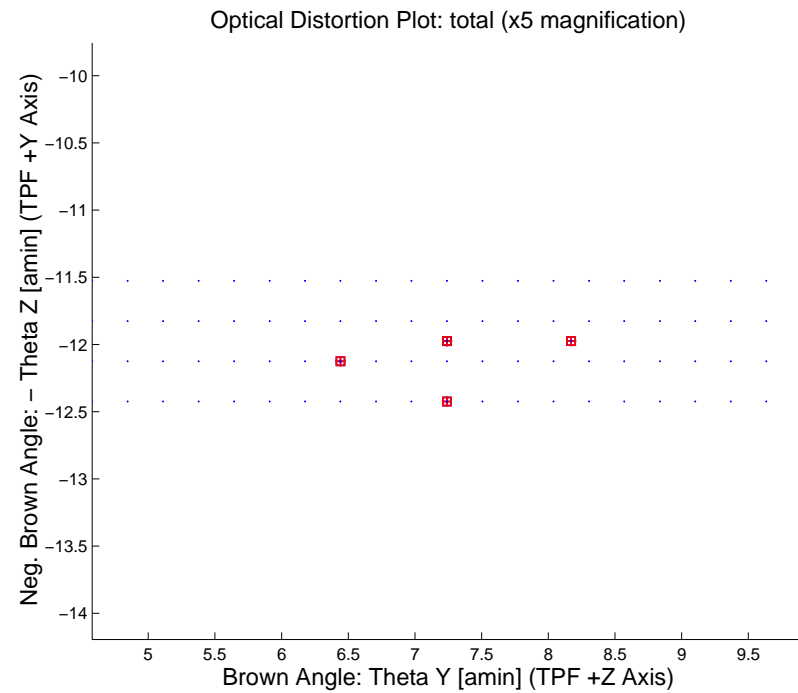


Figure 3.29: Optical Distortion Plot: total (x5 magnification)

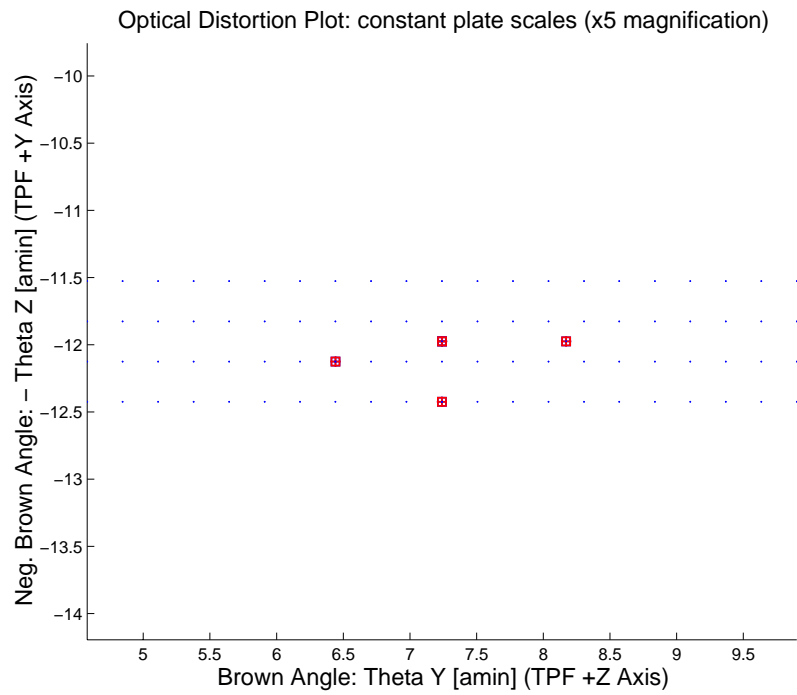


Figure 3.30: Optical Distortion Plot: constant plate scales (x5 magnification)

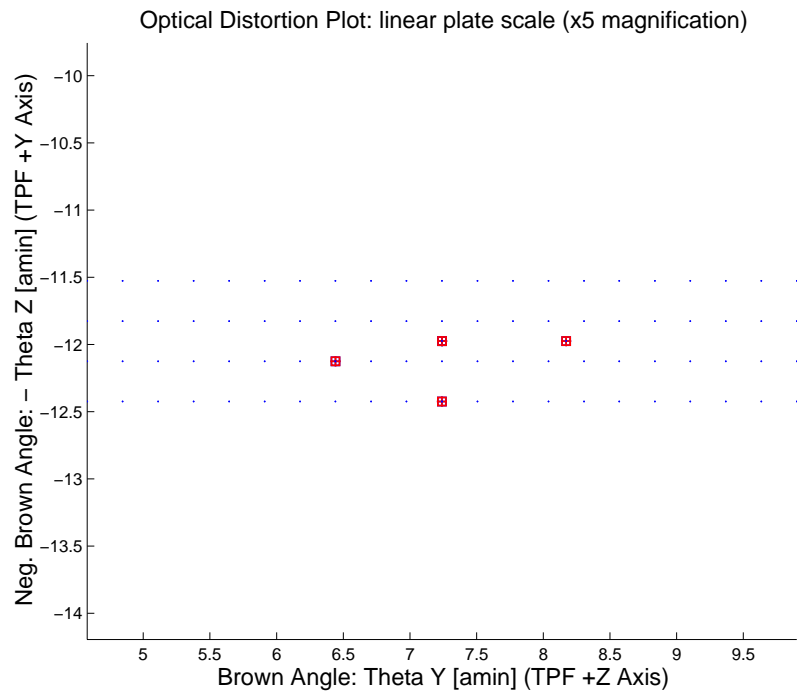


Figure 3.31: Optical Distortion Plot: linear plate scale (x5 magnification)

Opt. Dist. Plot:  $\Gamma$  depdt;  $\Gamma = 0.00000e+00$  in blue and  $\Gamma = 0.00000e+00$  in red (x5 magn)

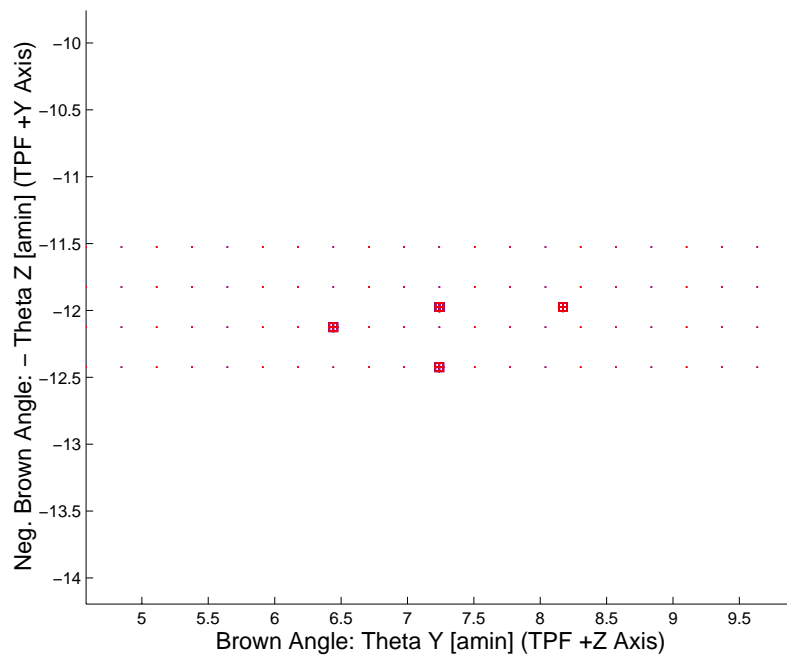


Figure 3.32: Optical Distortion Plot: gamma terms (x5 magnification)

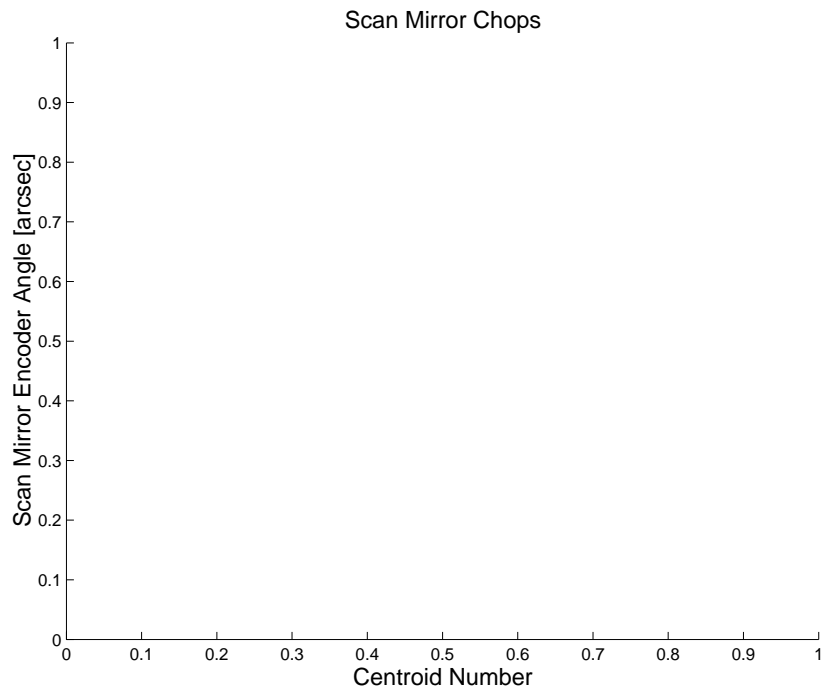


Figure 3.33: Scan Mirror Chops

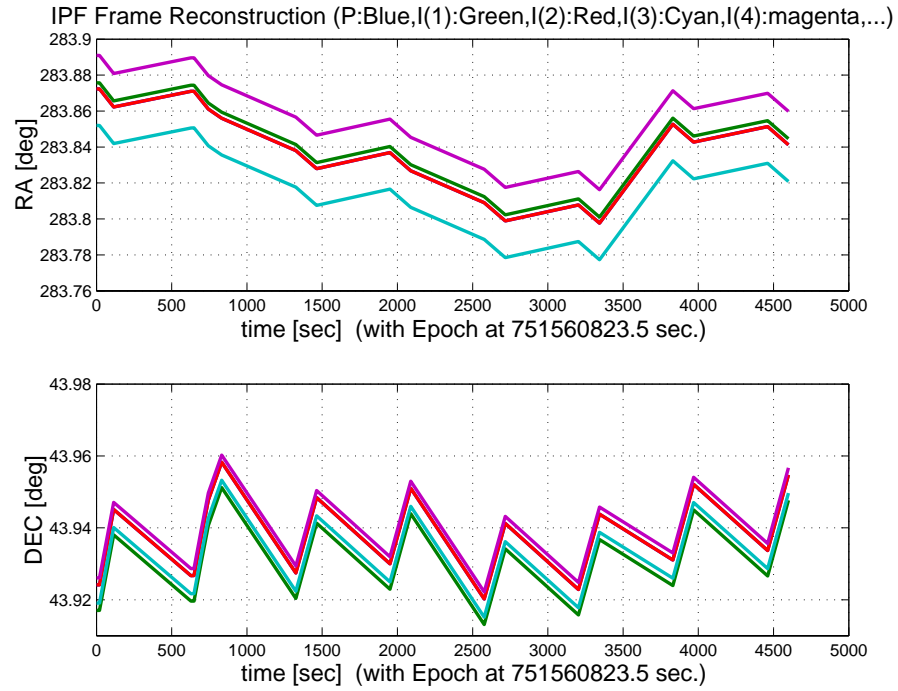


Figure 3.34: IPF Frame Reconstruction

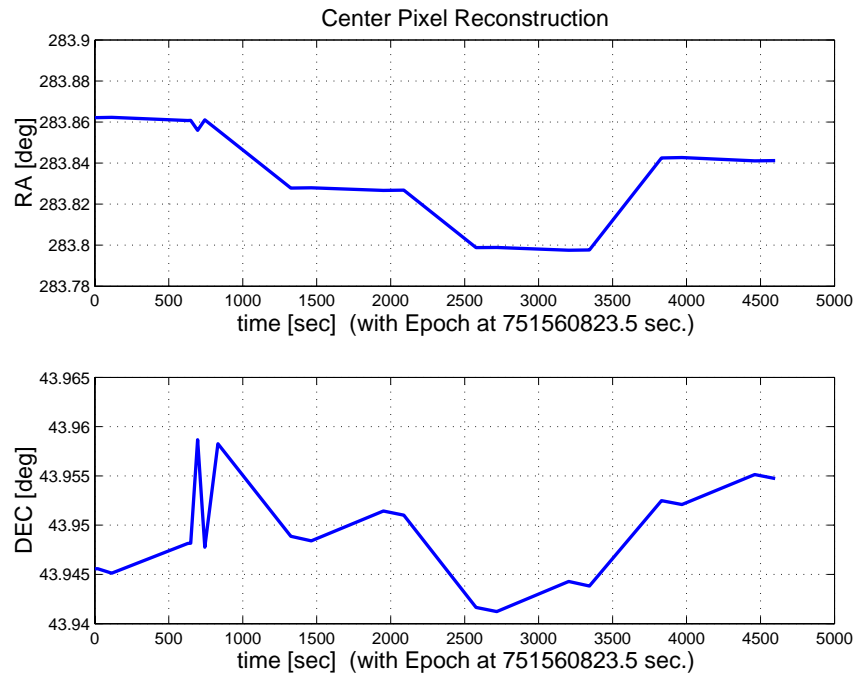


Figure 3.35: Center Pixel Reconstruction

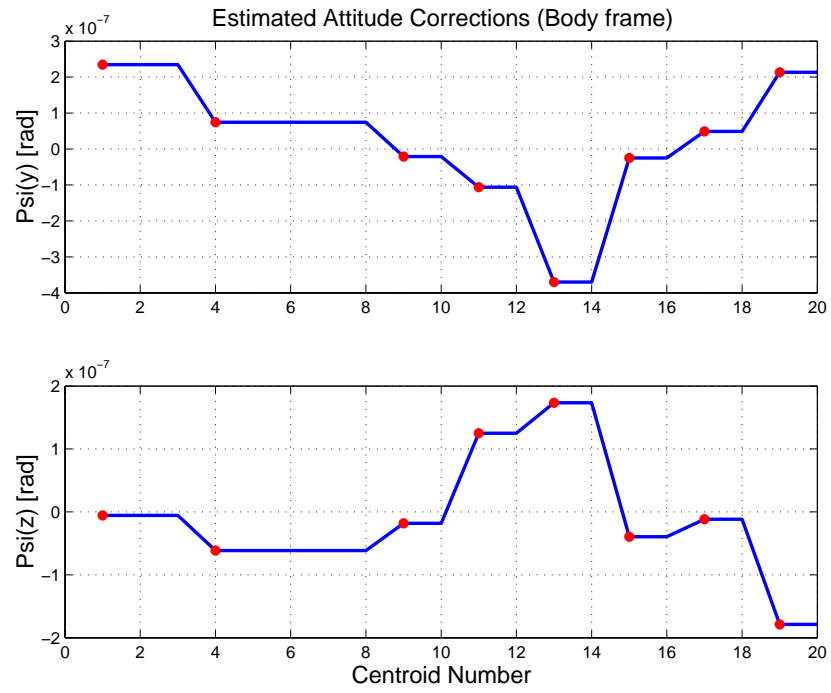


Figure 3.36: Estimated attitude corrections (Body frame)

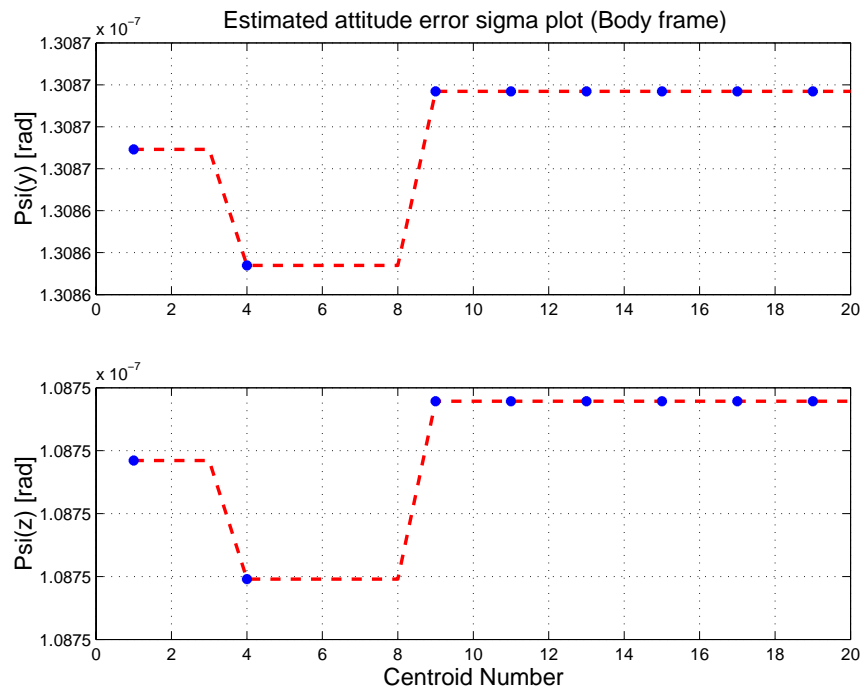


Figure 3.37: Estimated attitude error sigma plot (Body frame)

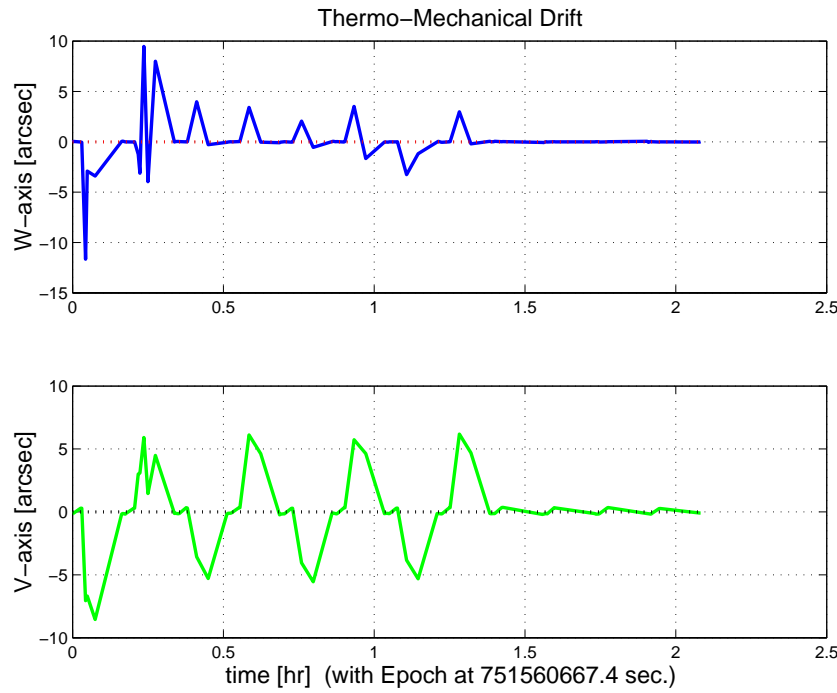


Figure 3.38: Thermo-mechanical boresight drift (equiv. angle in (W,V) coords)

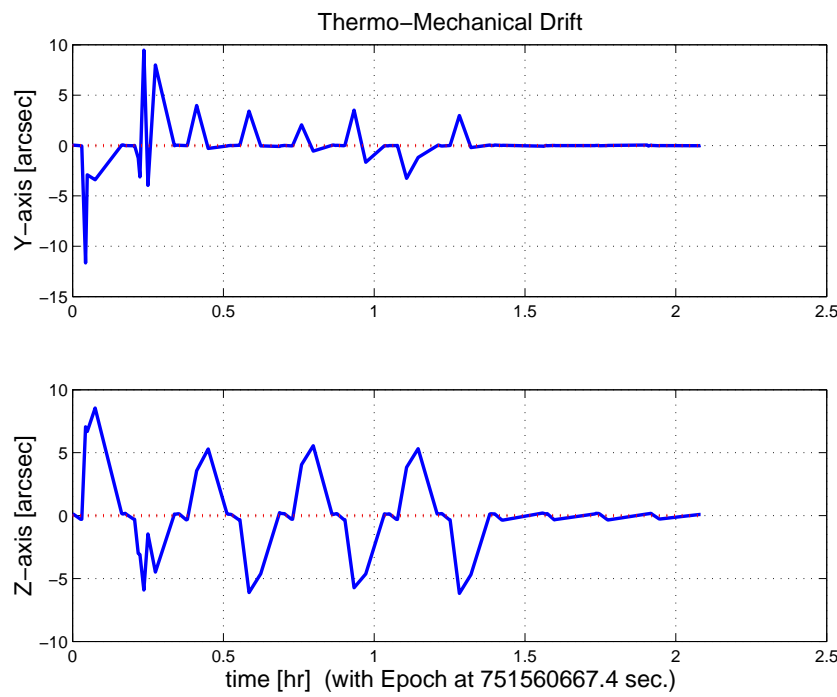


Figure 3.39: Thermo-mechanical boresight drift (equiv. angle in Body frame)

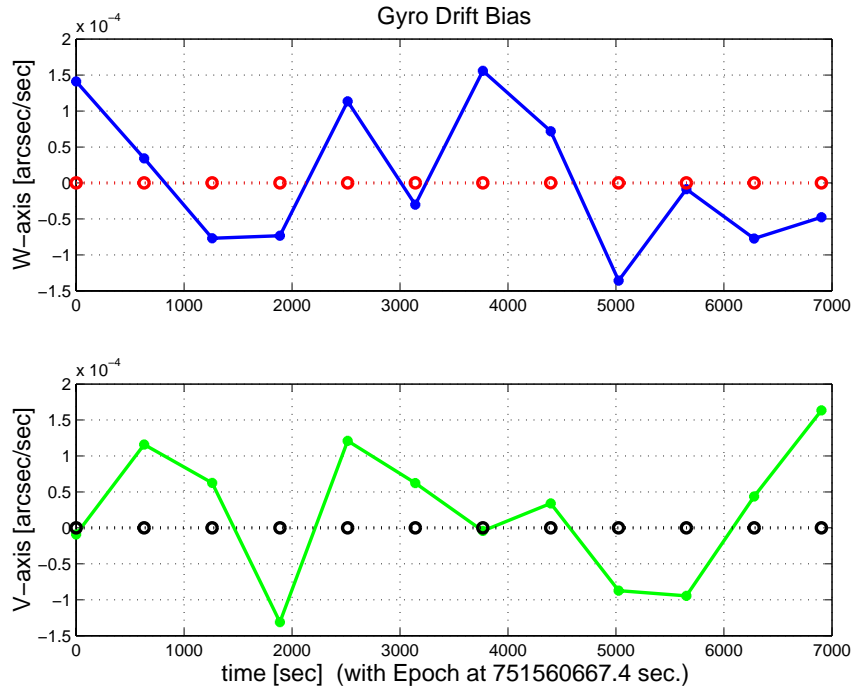


Figure 3.40: Gyro drift bias contribution (equiv. rate in (W,V) coords)

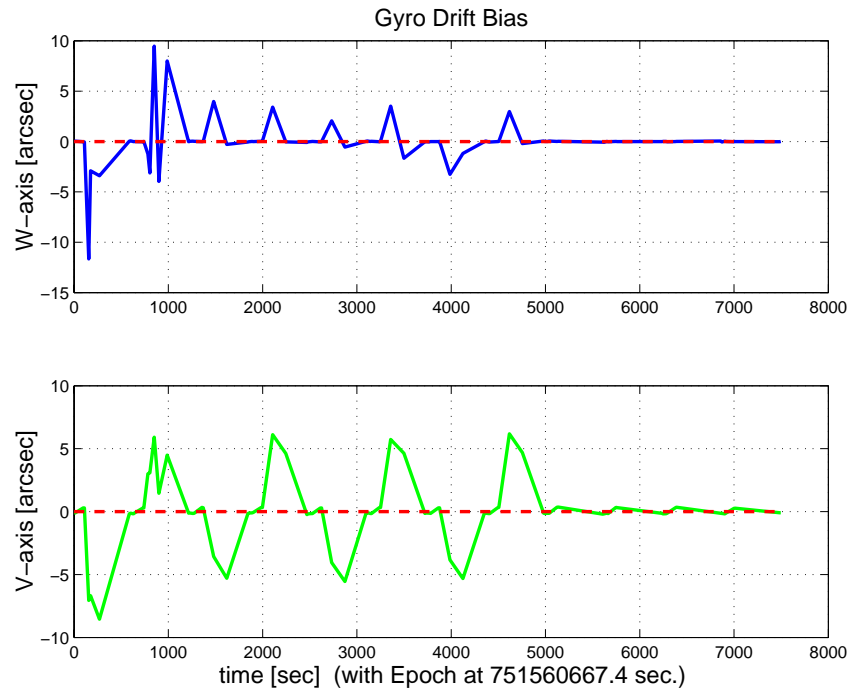


Figure 3.41: Gyro drift bias contribution (equiv. angle in (W,V) coords)

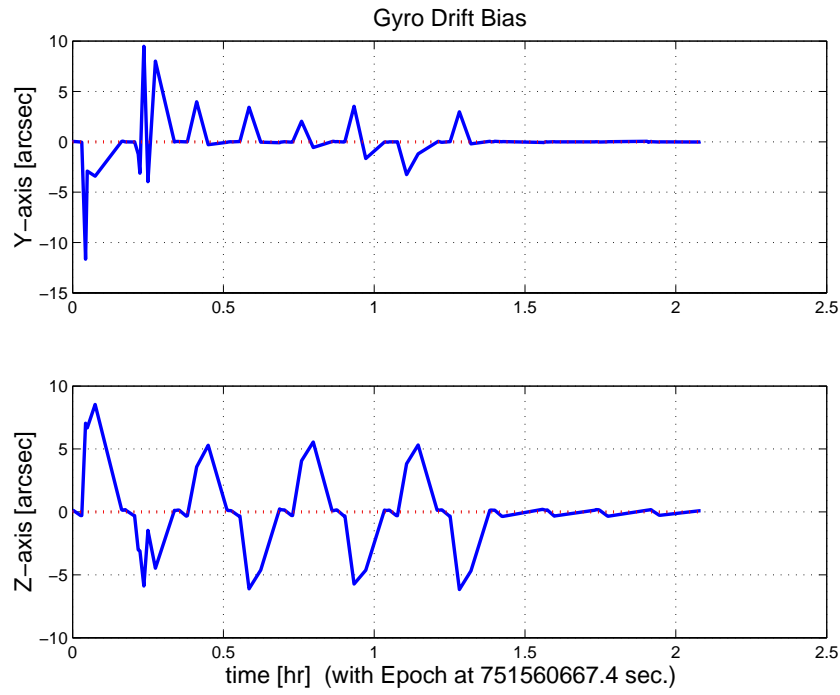


Figure 3.42: Gyro drift bias contribution (equiv. angle in Body frame)

### 3.2 IPF OUTPUT DATA (IF MINI FILE)

OUTPUT FILE NAME: IFmini103087.dat DATE: 27-Oct-2003 TIME: 23:08  
 INSTRUMENT NAME: MIPS\_160um\_center\_large\_FOV NF: 87  
 IPF FILTER VERSION: IPF.V2.0.0D SW RELEASE DATE: August 1, 2003  
 FRAME TABLE USED: BodyFrames\_FTU\_11a

---

----- IPF BROWN ANGLE SUMMARY -----

----- WAS -----			----- IS -----			
Frame Number	theta_Y (arcmin)	theta_Z (arcmin)	angle (deg)	theta_Y (arcmin)	theta_Z (arcmin)	angle (deg)
087	+6.720661	+11.925107	+0.000000	+7.240265	+11.975320	+0.000002
088	+6.715660	+12.382106	-0.000000	+7.240265	+12.424391	+0.000002
089	+6.720661	+11.925107	+0.000000	+7.240265	+11.975320	+0.000002
091	+7.640661	+11.954106	+0.000000	+8.171550	+11.975320	+0.000002
092	+5.930660	+12.034106	-0.000000	+6.442022	+12.125011	+0.000002

---

OFFSET	NF	Delta_CW	Delta_CV
0	87	+0.000	+0.000 pixels

OFFSET FRAME NAME: MIPS\_160um\_center\_large\_FOV

Brown Angle	theta_Y(arcmin)	theta_Z(arcmin)	angle(deg)
WAS(FTB)	+6.720661	+11.925107	+0.000000
IS (EST)	+7.240265	+11.975320	+0.000002
dT_EST	+0.519605	+0.050214	+0.000002
T_sSIGMA	+0.038505	+0.049966	+999.999999
dT_EST/T_sSIGMA	+13.494319	+1.004965	+999.999999

---

OFFSET	NF	Delta_CW	Delta_CV
1	88	+0.000	-1.500 pixels

OFFSET FRAME NAME: MIPS\_160um\_plusY\_edge

Brown Angle	theta_Y(arcmin)	theta_Z(arcmin)	angle(deg)
WAS(FTB)	+6.715660	+12.382106	-0.000000
IS (EST)	+7.240265	+12.424391	+0.000002
dT_EST	+0.524605	+0.042285	+0.000002
T_sSIGMA	+0.038505	+0.049966	+999.999999
dT_EST/T_sSIGMA	+13.624169	+0.846279	+999.999999

---

OFFSET	NF	Delta_CW	Delta_CV
2	89	+0.000	+0.000 pixels

OFFSET FRAME NAME: MIPS\_160um\_large\_only

Brown Angle	theta_Y(arcmin)	theta_Z(arcmin)	angle(deg)
WAS(FTB)	+6.720661	+11.925107	+0.000000
IS (EST)	+7.240265	+11.975320	+0.000002
dT_EST	+0.519605	+0.050214	+0.000002
T_sSIGMA	+0.038505	+0.049966	+999.999999
dT_EST/T_sSIGMA	+13.494319	+1.004965	+999.999999

---

OFFSET	NF	Delta_CW	Delta_CV
3	91	+3.500	+0.000 pixels

OFFSET FRAME NAME: MIPS\_160um\_small\_FOV1

Brown Angle	theta_Y(arcmin)	theta_Z(arcmin)	angle(deg)
WAS(FTB)	+7.640661	+11.954106	+0.000000
IS (EST)	+8.171550	+11.975320	+0.000002
dT_EST	+0.530889	+0.021214	+0.000002
T_sSIGMA	+0.038505	+0.049966	+999.999999
dT_EST/T_sSIGMA	+13.787377	+0.424567	+999.999999

---

OFFSET	NF	Delta_CW	Delta_CV
4	92	-3.000	-0.500 pixels

OFFSET FRAME NAME: MIPS\_160um\_small\_FOV2

Brown Angle	theta_Y(arcmin)	theta_Z(arcmin)	angle(deg)
WAS(FTB)	+5.930660	+12.034106	-0.000000
IS (EST)	+6.442022	+12.125011	+0.000002
dT_EST	+0.511361	+0.090904	+0.000002

T_sSIGMA	+0.038505	+0.049966	+999.999999
dT_EST/T_sSIGMA	+13.280226	+1.819330	+999.999999

---

VARNAME	MEAN	SIGMA	SCALED_SIGMA
del_theta2	-1.1524113203605046E-017	+4.5039835969604530E-006	+1.1200780636607969E-005
del_theta3	+1.4575053914901744E-017	+5.8444853832678163E-006	+1.4534422096035723E-005
del_arx	+3.1162617415193567E-016	+1.3505133327351838E-005	+3.3585387826433421E-005
del_ary	-1.4315932143393995E-018	+1.3990370113048806E-006	+3.4792104209031342E-006
del_arz	+9.6681697175810428E-020	+1.3991140721385510E-006	+3.4794020604762002E-006

---

LSQF RESIDUAL SIGMA SCALE =	+2.4868608855873497E+000
-----------------------------	--------------------------

---

	qT(1)	qT(2)	qT(3)	qT(4)
FrmTbl:	-1.6953765806708300E-006	-9.7747882102736799E-004	-1.7344347357590400E-003	+9.999801813224998E-001
Estim:	-1.8193149813468925E-006	-1.0530521324111316E-003	-1.7417378662919617E-003	+9.999792871140569E-001
DelTheta	deltheta(1)	deltheta(2)	deltheta(3)	
	+1.1038964626866072E-009	-1.5114690333173922E-004	-1.4606556388790096E-005	[rad]
EulAngT	theta(1)	theta(2)	theta(3)	[rad]
Mean	+2.9659188138343540E-008	-2.1061077970186636E-003	-3.4834794565500385E-003	
SigmaT	+9.9999000000000000E+004	+4.5039835969604530E-006	+5.8444853832678163E-006	

---

	qR(1)	qR(2)	qR(3)	qR(4)
ASFILE:	+7.0910510839894414E-004	+1.2698431964963675E-003	-1.6105116810649633E-004	+9.999892711639404E-001
Estim:	+6.7596050461530904E-004	+1.2696723544321671E-003	-1.6084665716067665E-004	+9.999895256838212E-001
DelThetaR	delthetaR(1)	delthetaR(2)	delthetaR(3)	
	-6.6289637126397039E-005	-3.5212354206236793E-007	+3.2510671366220477E-007	[rad]
EulAngR	angR(1)	angR(2)	angR(3)	[rad]
Mean	+1.3515159177371146E-003	+2.5395622308140181E-003	-3.1997751792613285E-004	
SigmaR	+1.3505133327351838E-005	+1.3990370113048806E-006	+1.3991140721385510E-006	

---

Initial Gyro Bias	Bg0(1)	Bg0(2)	Bg0(3)
	+0.0000000000000000E+000	+0.0000000000000000E+000	+0.0000000000000000E+000
Gyro Bias Correction	Bg(1)	Bg(2)	Bg(3)
	+0.0000000000000000E+000	+0.0000000000000000E+000	+0.0000000000000000E+000
Total Gyro Bias	BgT(1)	BgT(2)	BgT(3)
	+0.0000000000000000E+000	+0.0000000000000000E+000	+0.0000000000000000E+000

---

Initial Gyro Bias Rate	Cg0(1)	Cg0(2)	Cg0(3)
	+0.0000000000000000E+000	+0.0000000000000000E+000	+0.0000000000000000E+000
Gyro Bias Rate Correction	Cg(1)	Cg(2)	Cg(3)
	+0.0000000000000000E+000	+0.0000000000000000E+000	+0.0000000000000000E+000
Total Gyro Bias Rate	CgT(1)	CgT(2)	CgT(3)
	+0.0000000000000000E+000	+0.0000000000000000E+000	+0.0000000000000000E+000

---

OFFSET	NF	Delta_CW	Delta_CV
1	88	+0.000	-1.500 pixels

OFFSET FRAME NAME: MIPS\_160um\_plusY\_edge

	qT(1)	qT(2)	qT(3)	qT(4)
WAS(FTB)	-1.7590379425356295E-006	-9.7675148718468288E-004	-1.8009025571078395E-003	+9.9999790134950672E-001
IS (EST)	-1.8880947946946152E-006	-1.0530520004150405E-003	-1.8070524774803842E-003	+9.9999781281723976E-001

---

DelTheta	deltheta(1)	deltheta(2)	deltheta(3)
Units	rad	rad	rad
	+5.6307265787403232E-009	-1.5260132247061150E-004	-1.2300150591555674E-005
EulAngT	theta(1)	theta(2)	theta(3)
Mean	+2.9659188138343540E-008	-2.1061077751749792E-003	-3.6141089570213966E-003
sSigmaT	+1.4631491302441851E-009	+1.1200780536791504E-005	+1.4534422099312058E-005
SigmaT	+5.8835182085330709E-010	+4.5039835568229184E-006	+5.8444853845852744E-006

---

OFFSET	NF	Delta_CW	Delta_CV
2	89	+0.000	+0.000 pixels

OFFSET FRAME NAME: MIPS\_160um\_large\_only

qT	qT(1)	qT(2)	qT(3)	qT(4)
WAS(FTB)	-1.6953765806708300E-006	-9.7747882102736799E-004	-1.7344347357590400E-003	+9.9999801813224998E-001
IS (EST)	-1.8193149813468923E-006	-1.0530521324111314E-003	-1.7417378662919617E-003	+9.9999792871140569E-001

---

DelTheta	deltheta(1)	deltheta(2)	deltheta(3)	
Units	rad	rad	rad	
	+1.1038964626861806E-009	-1.511469033173879E-004	-1.4606556388790096E-005	
EulAngT	theta(1)	theta(2)	theta(3)	[rad]
Mean	+2.9659188138343540E-008	-2.1061077970186636E-003	-3.4834794565500381E-003	
sSigmaT	+8.7609742638596906E-024	+1.1200780636607969E-005	+1.4534422096035723E-005	
SigmaT	+3.5229048454757105E-024	+4.5039835969604530E-006	+5.8444853832678163E-006	

---

OFFSET	NF	Delta_CW	Delta_CV
3	91	+3.500	+0.000 pixels

OFFSET FRAME NAME: MIPS\_160um\_small\_FOV1

qT	qT(1)	qT(2)	qT(3)	qT(4)
WAS(FTB)	-1.9321460815626504E-006	-1.1112871145329802E-003	-1.7386523634373104E-003	+9.9999787106032123E-001
IS (EST)	-2.0552330507836398E-006	-1.1885016602688854E-003	-1.7417376038885589E-003	+9.9999777690237834E-001

---

DelTheta	deltheta(1)	deltheta(2)	deltheta(3)	
Units	rad	rad	rad	
	+1.5944028868706793E-008	-1.5442938816823159E-004	-6.1708212409321880E-006	
EulAngT	theta(1)	theta(2)	theta(3)	[rad]
Mean	+2.9659188138343540E-008	-2.3770074339938617E-003	-3.4834794645847243E-003	
sSigmaT	+3.9373696213019972E-009	+1.1200780636607967E-005	+1.4534421562719718E-005	
SigmaT	+1.5832689492689755E-009	+4.5039835969604521E-006	+5.8444851688143232E-006	

---

OFFSET	NF	Delta_CW	Delta_CV
4	92	-3.000	-0.500 pixels

OFFSET FRAME NAME: MIPS\_160um\_small\_FOV2

qT	qT(1)	qT(2)	qT(3)	qT(4)
WAS(FTB)	-1.5097633610600495E-006	-8.6257817629657057E-004	-1.7502882965202491E-003	+9.9999809622193259E-001
IS (EST)	-1.6374983930801738E-006	-9.3695248391687381E-004	-1.7635095956557089E-003	+9.9999800607364597E-001

---

DelTheta	deltheta(1)	deltheta(2)	deltheta(3)	
Units	rad	rad	rad	
	-1.5959024152503599E-008	-1.4874889516147951E-004	-2.644286600332051E-005	
EulAngT	theta(1)	theta(2)	theta(3)	[rad]
Mean	+2.9659188138343540E-008	-1.8739081036078934E-003	-3.5270225954128474E-003	
sSigmaT	+3.4104601491445876E-009	+1.1200780624572429E-005	+1.4534421705183457E-005	
SigmaT	+1.3713916081554763E-009	+4.5039835921208015E-006	+5.8444852261008961E-006	

---

q(1)	q(2)	q(3)	q(4)	
PCRS1A:	+5.337188965461637E-007	+3.7444233778550031E-004	-1.4253684912431913E-003	+9.9999891405806784E-001
PCRS2A:	-5.2779261998836216E-007	+3.8462959425181312E-004	+1.3722087221825403E-003	+9.9999898455099423E-001

---

\*\*\*\*\* CS-FILE PARAMETERS: \*\*\*\*\* AS-FILE PARAMETERS: \*\*\*\*\*

Row (01) PIX2RADX:	+7.739989817200000E-005	Row (1) TASTART:	+7.5156000029075623E+008
Row (02) PIX2RADY:	+8.708614099900005E-005	Row (2) TASTOP:	+7.5156900019077146E+008
Row (03) CX0:	+1.050000000000000E+001	Row (3) S/C TIME:	+7.5155940039074707E+008
Row (04) CY0:	+2.000000000000000E+000	Row (4) QR1:	+7.0910510839894414E-004
Row (05) BETA0:	+2.804741000000001E-006	Row (5) QR2:	+1.2698431964963675E-003
Row (06) GAMMA_E0:	+2.007000000000000E+003	Row (6) QR3:	-1.6105116810649633E-004
Row (07) D11:	-1.000000000000000E+000	Row (7) QR4:	+9.9999892711639404E-001
Row (08) D12:	+0.000000000000000E+000		
Row (09) D21:	+0.000000000000000E+000		
Row (10) D22:	-1.000000000000000E+000		
Row (11) DG:	-1.000000000000000E+000		

---

INITIAL STA-TO-PCRS ALIGNMENT (R) KNOWLEDGE (1-SIGMA)

SIGMA(X)	SIGMA(Y)	SIGMA(Z)
5.93701930E+000	3.91099423E-001	3.91310719E-001

[arcsec]

---

PIX2RADX = 7.739989817200E-005 [rad/pixel]

```

XPIXSIZE = 15.9649[arcsec]
PIX2RADY = 8.708614099900E-005[rad/pixel]
YPIXSIZE = 17.9628[arcsec]
CX0 = 10.5[pixel] = 167.63[arcsec]
CY0 = 2.0[pixel] = 35.93[arcsec]
-----
NOMINAL BETA0 = 2.804741000000E-006[rad/encoder unit]
ENCODER UNIT SIZE = 0.58[arcsec]
GAMMA_E0 = 2007.00[encoder unit] = 1161.09[arcsec]
-----
| -1 | +0 |
FLIP MATRIX D = |----|----| and DG = -1
| +0 | -1 |
-----

```

### 3.3 IPF EXECUTION LOG

```

*****
IPF EXECUTION-LOG FILE NAME: LG103087.dat
INSTRUMENT TYPE: MIPS_160um_center_large_FOV
IPF FILTER EXECUTION DATE: 27-Oct-2003 TIME: 23:07
IPF FILTER VERSION USED: IPF.V2.0.0D
*****



----- Loading & Preparing Input Files -----
AAFILE: AA101087 Loaded! AAFILE dimension = 90000 X 21
ASFILE: AS101087 Loaded!
CAFFILE: CA191087 Loaded! CAFFILE dimension = 20 X 15
CBFILE: CB101087 Loaded! CBFILE dimension = 72 X 15
CCFILE: CC103087 Created! CCFILE dimension = 92 X 19
CSFILE: CS102087 Loaded!
Loading Input Files Completed!
-----



----- Selected Mask Vectors -----
index = 1 2 3 4 5 6 7 8 9 10 11 12 13 14 15 16 17 18 19 20
-----
mask1 = [ 0 0 0 0 0 0 0 0 0 0 0 0 0 0 0 0 0 0 0 0 ]
mask2 = [ 0 0 0 1 1 1 1 0 0 0 0 0 0 0 0 0 0 0 0 0 ]
-----



----- Selected Initial Gyro Bias Parameters -----
IPF Filter in LITE MODE# 3
IPF LITE MODE WITH FILTERED STA QUATERNION!
IPF Linearized Using Following Nominal Gyro Bias Estimates
bg0 = [+0.00000000000000E+000 +0.00000000000000E+000 +0.00000000000000E+000 ]
cg0 = [+0.00000000000000E+000 +0.00000000000000E+000 +0.00000000000000E+000 ]
-----



----- Gyro Pre-Processor Run Completed -----
AGFILE CREATED: AG103087.m ACFILE CREATED: AC103087.m
-----



Total Gyro Preprocessor Execution Time: 2 seconds

FRAME TABLE ENTRIES FOR PCRS LOADED TO TPCRS
q_PCRS4 = [ +5.3371888965461637E-007 q_PCRS5 = [ +7.3379987833742897E-007
            +3.7444233778550031E-004 +5.2236196154513707E-004
            -1.4253684912431913E-003 -1.4047712280184723E-003
            +9.9999891405806784E-001 ]; +9.9999887687698918E-001 ];
q_PCRS8 = [ -5.2779261998836216E-007 q_PCRS9 = [ -7.1963421681856818E-007

```

```

+3.8462959425181312E-004          +5.3239763239987400E-004
+1.3722087221825403E-003          +1.3516841804518383E-003
+9.9999898455099423E-001 ] ;      +9.9999894475050310E-001 ] ;

----- Initial Conditions for State ----- ----- Initial Square-Root Cov (diag) -----
p1(01) = a00 = +0.0000000000000000E+000 Sigma_initial(01,01) = 9.9999000000000000E+004
p1(02) = b00 = +0.0000000000000000E+000 Sigma_initial(02,02) = 9.9999000000000000E+004
p1(03) = c00 = +0.0000000000000000E+000 Sigma_initial(03,03) = 9.9999000000000000E+004
p1(04) = a10 = +0.0000000000000000E+000 Sigma_initial(04,04) = 9.9999000000000000E+004
p1(05) = b10 = +0.0000000000000000E+000 Sigma_initial(05,05) = 9.9999000000000000E+004
p1(06) = c10 = +0.0000000000000000E+000 Sigma_initial(06,06) = 9.9999000000000000E+004
p1(07) = d10 = +0.0000000000000000E+000 Sigma_initial(07,07) = 9.9999000000000000E+004
p1(08) = a20 = +0.0000000000000000E+000 Sigma_initial(08,08) = 9.9999000000000000E+004
p1(09) = b20 = +0.0000000000000000E+000 Sigma_initial(09,09) = 9.9999000000000000E+004
p1(10) = c20 = +0.0000000000000000E+000 Sigma_initial(10,10) = 9.9999000000000000E+004
p1(11) = d20 = +0.0000000000000000E+000 Sigma_initial(11,11) = 9.9999000000000000E+004
p1(12) = a01 = +0.0000000000000000E+000 Sigma_initial(12,12) = 9.9999000000000000E+004
p1(13) = b01 = +0.0000000000000000E+000 Sigma_initial(13,13) = 9.9999000000000000E+004
p1(14) = c01 = +0.0000000000000000E+000 Sigma_initial(14,14) = 9.9999000000000000E+004
p1(15) = d01 = +0.0000000000000000E+000 Sigma_initial(15,15) = 9.9999000000000000E+004
p1(16) = e01 = +0.0000000000000000E+000 Sigma_initial(16,16) = 9.9999000000000000E+004
p1(17) = f01 = +0.0000000000000000E+000 Sigma_initial(17,17) = 9.9999000000000000E+004

----- p2f(01) = am1 = +0.0000000000000000E+000 Sigma_initial(18,18) = 9.9999000000000000E+004
p2f(02) = am2 = +0.0000000000000000E+000 Sigma_initial(19,19) = 9.9999000000000000E+004
p2f(03) = am3 = +1.0000000000000000E+000 Sigma_initial(20,20) = 9.9999000000000000E+004
p2f(04) = beta = +1.0000000000000000E+000 Sigma_initial(21,21) = 1.0000000000000000E-002
p2f(05) = qT1 = -1.6953765806708300E-006 Sigma_initial(22,22) = 1.0000000000000000E-002
p2f(06) = qT2 = -9.7747882102736799E-004
p2f(07) = aT3 = -1.7344347357590400E-003
p2f(08) = qT4 = +9.9999801813224998E-001
p2f(09) = qR1 = +7.0910510839894414E-004
p2f(10) = qR2 = +1.2698431964963675E-003
p2f(11) = qR3 = -1.6105116810649633E-004
p2f(12) = qR4 = +9.9999892711639404E-001
p2f(13) = brx = +0.0000000000000000E+000
p2f(14) = bry = +0.0000000000000000E+000
p2f(15) = brz = +0.0000000000000000E+000
p2f(16) = crx = +0.0000000000000000E+000
p2f(17) = cry = +0.0000000000000000E+000
p2f(18) = crz = +0.0000000000000000E+000
p2f(19) = bgx = +0.0000000000000000E+000
p2f(20) = bgy = +0.0000000000000000E+000
p2f(21) = bgz = +0.0000000000000000E+000
p2f(22) = cgx = +0.0000000000000000E+000
p2f(23) = cgy = +0.0000000000000000E+000
p2f(24) = cgz = +0.0000000000000000E+000

----- IPF KALMAN FILTER STARTED -----
Iteration#001: |dp|= +1.656433646278E-004 RMS(|Res|)=+1.559773292974E-004
Iteration#002: |dp|= +2.637358062106E-007 RMS(|Res|)=+3.344689159209E-005
Iteration#003: |dp|= +1.4468893363887E-007 RMS(|Res|)=+3.344690167248E-005
Iteration#004: |dp|= +1.180008962926E-009 RMS(|Res|)=+3.344689628297E-005
Iteration#005: |dp|= +3.143612304814E-010 RMS(|Res|)=+3.344689620981E-005
Iteration#006: |dp|= +3.932836289537E-012 RMS(|Res|)=+3.344689622763E-005
Iteration#007: |dp|= +6.832936856423E-013 RMS(|Res|)=+3.344689622812E-005
Iteration#008: |dp|= +1.177587837555E-014 RMS(|Res|)=+3.344689622804E-005
Iteration#009: |dp|= +2.490248972427E-015 RMS(|Res|)=+3.344689622805E-005
Iteration#010: |dp|= +1.343129215704E-015 RMS(|Res|)=+3.344689622804E-005
Iteration#011: |dp|= +1.849159299681E-015 RMS(|Res|)=+3.344689622803E-005
Iteration#012: |dp|= +2.168314271828E-016 RMS(|Res|)=+3.344689622803E-005
Iteration#013: |dp|= +1.136693602661E-016 RMS(|Res|)=+3.344689622805E-005
Iteration#014: |dp|= +6.178778021061E-016 RMS(|Res|)=+3.344689622803E-005
Iteration#015: |dp|= +1.242704756857E-015 RMS(|Res|)=+3.344689622804E-005
Iteration#016: |dp|= +2.165281446929E-015 RMS(|Res|)=+3.344689622804E-005
Iteration#017: |dp|= +1.749510105104E-015 RMS(|Res|)=+3.344689622804E-005
Iteration#018: |dp|= +9.216076449477E-017 RMS(|Res|)=+3.344689622802E-005

```

```

Iteration#019: |dp|= +6.261616922021E-016 RMS(|Res|)=+3.344689622804E-005
Iteration#020: |dp|= +3.918251949989E-016 RMS(|Res|)=+3.344689622802E-005
Iteration#021: |dp|= +2.189371162780E-016 RMS(|Res|)=+3.344689622803E-005
Iteration#022: |dp|= +1.236262402462E-015 RMS(|Res|)=+3.344689622804E-005
Iteration#023: |dp|= +1.660437574098E-015 RMS(|Res|)=+3.344689622805E-005
Iteration#024: |dp|= +1.652521193377E-015 RMS(|Res|)=+3.344689622803E-005
Iteration#025: |dp|= +1.563143215235E-015 RMS(|Res|)=+3.344689622805E-005
Iteration#026: |dp|= +1.236009825087E-015 RMS(|Res|)=+3.344689622803E-005
Iteration#027: |dp|= +5.131948885929E-016 RMS(|Res|)=+3.344689622804E-005
Iteration#028: |dp|= +6.240121494273E-016 RMS(|Res|)=+3.344689622804E-005
Iteration#029: |dp|= +1.954141469122E-016 RMS(|Res|)=+3.344689622804E-005
Iteration#030: |dp|= +3.121829088929E-016 RMS(|Res|)=+3.344689622804E-005
IPF Kalman Filter Completed with Error |dp1| + |dp2| = +3.1218290889285763E-016
-----
```

```

----- IPF LEAST SQUARES FILTER STARTED -----
Iteration#001 COND#=+9.657438676443E+000, |dp|=+1.657014294671E-004
Iteration#002 COND#=+9.657439161173E+000, |dp|=+3.203994688909E-008
Iteration#003 COND#=+9.657439160941E+000, |dp|=+1.548112484682E-011
Iteration#004 COND#=+9.657439160941E+000, |dp|=+6.077273033442E-015
Iteration#005 COND#=+9.657439160941E+000, |dp|=+1.993799307089E-015
Iteration#006 COND#=+9.657439160941E+000, |dp|=+4.426033407719E-016
Iteration#007 COND#=+9.657439160941E+000, |dp|=+1.919537466004E-015
Iteration#008 COND#=+9.657439160941E+000, |dp|=+5.652664566786E-016
Iteration#009 COND#=+9.657439160941E+000, |dp|=+3.553028439317E-016
Iteration#010 COND#=+9.657439160941E+000, |dp|=+1.093384457454E-015
Iteration#011 COND#=+9.657439160941E+000, |dp|=+2.009688449016E-015
Iteration#012 COND#=+9.657439160941E+000, |dp|=+1.355482057641E-016
Iteration#013 COND#=+9.657439160941E+000, |dp|=+8.885869395679E-016
Iteration#014 COND#=+9.657439160941E+000, |dp|=+5.605217576325E-016
Iteration#015 COND#=+9.657439160941E+000, |dp|=+1.301139801055E-015
Iteration#016 COND#=+9.657439160941E+000, |dp|=+3.786700185573E-016
Iteration#017 COND#=+9.657439160941E+000, |dp|=+7.678892540305E-016
Iteration#018 COND#=+9.657439160941E+000, |dp|=+1.406963904736E-015
Iteration#019 COND#=+9.657439160941E+000, |dp|=+2.008819816802E-015
Iteration#020 COND#=+9.657439160941E+000, |dp|=+7.882057421169E-016
Iteration#021 COND#=+9.657439160941E+000, |dp|=+4.592875180032E-016
Iteration#022 COND#=+9.657439160941E+000, |dp|=+6.763492708809E-016
Iteration#023 COND#=+9.657439160941E+000, |dp|=+2.835021366480E-016
Iteration#024 COND#=+9.657439160941E+000, |dp|=+9.602550749541E-016
Iteration#025 COND#=+9.657439160941E+000, |dp|=+6.757099732253E-016
Iteration#026 COND#=+9.657439160941E+000, |dp|=+2.783947651777E-016
Iteration#027 COND#=+9.657439160941E+000, |dp|=+5.539881176710E-016
Iteration#028 COND#=+9.657439160941E+000, |dp|=+1.082580930623E-015
Iteration#029 COND#=+9.657439160941E+000, |dp|=+2.236221866199E-015
Iteration#030 COND#=+9.657439160941E+000, |dp|=+1.067091654290E-015
IPF Least Squares Filter Completed with Error |dp1| + |dp2| = +1.0670916542896194E-015
-----
```

Total Execution Time: 56 seconds

## 4 COMMENTS

Overall the science data appeared very inaccurate in the V direction. The filter, however, converged nicely after we removed 3 bad centroids and restricting the number of degrees of freedom.

1. A center pixel definition error in the V direction was detected when using file CS101087.m. A new CS file (CS102087.m) was re-delivered which fixed the problem. Centroids 3, 5 and 6 were removed because they were associated with large centroiding errors.
2. Science centroids appear collapsed to the center of each row of pixels indicating very poor centroiding performance along the V direction (dispersion). This suggests the need for an improved centroiding approach for the upcoming fine survey.
3. We estimated only 2 Brown angles (no Twist) because of the large uncertainty in the science centroids.
4. The IPF filter was run in Lite Mode 3 (Observer based) for robustness with respect to large science centroiding errors.
5. Our results show large systematic errors in PCRS a-posteriori residuals suggesting an incorrect relative distance between PCRS1 and PCRS2 in frame table FTU11a. This error is on the order of 0.45 arcsec. Consequently, an urgent PAC filter run is essential for achieving fine survey accuracies.
6. We also estimated the STA to PCRS alignment using the PCRS data.

We recommend updating the frame table entries for frames 87, 88, 89, 91 and 92 with the quaterninons given in IF103087.dat. The recommended corrections are on the order of 0.5 arcmin in the W direction and 3 arcsec in the V direction with a knowledge error of about 3.8 arcsec. While this knowledge error is larger than the desired Coarse Survey accuracy of 3.75 arcsec. This is due to fewer and less accurate than expected science centroids as well as the systematic errors in PCRS.

## IPF TEAM CONTACT INFORMATION

IPF Team email	ipf@sirtfweb.jpl.nasa.gov	
David S. Bayard	X4-8208	David.S.Bayard@jpl.nasa.gov (TEAM LEADER)
Dhemetrio Boussalis	X4-3977	boussali@grover.jpl.nasa.gov
Paul Brugarolas	X4-9243	Paul.Brugarolas@jpl.nasa.gov
Bryan H. Kang	X4-0541	Bryan.H.Kang@jpl.nasa.gov
Edward.C.Wong	X4-3053	Edward.C.Wong@jpl.nasa.gov (TASK MANAGER)

## ACKNOWLEDGEMENTS

This work was performed at the Jet Propulsion Laboratory, California Institute of Technology, under contract with the National Aeronautics and Space Administration.

## References

- [1] D.S. Bayard, B.H. Kang, *SIRTF Instrument Pointing Frame Kalman Filter Algorithm*, JPL D-Document D-24809, September 30, 2003.
- [2] B.H. Kang, D.S. Bayard, *SIRTF Instrument Pointing Frame (IPF) Software Description Document and User's Guide*, JPL D-Document D-24808, September 30, 2003.
- [3] D.S. Bayard, B.H. Kang, *SIRTF Instrument Pointing Frame (IPF) Kalman Filter Unit Test Report*, JPL D-Document D-24810, September 30, 2003.
- [4] *Space Infrared Telescope Facility In-Orbit Checkout and Science Verification Mission Plan*, JPL D-Document D-22622, 674-FE-301 Version 1.4, February 8, 2002.
- [5] *Space Infrared Telescope Facility Observatory Description Document*, Lockheed Martin LMMS/P458569, 674-SEIT-300 Version 1.2, November 1, 2002.
- [6] *SIRTF Software Interface Specification for Science Centroid INPUT Files (CAFILe, CS-FILE)*, JPL SOS-SIS-2002, November 18, 2002.
- [7] *SIRTF Software Interface Specification for Inferred Frames Offset INPUT Files (OFILE)*, JPL SOS-SIS-2003, November 18, 2002.
- [8] *SIRTF Software Interface Specification for PCRS Centroid INPUT Files (CBFILE)*, JPL SIS-FES-015, November 18, 2002.
- [9] *SIRTF Software Interface Specification for Attitude INPUT Files (AFILE, ASFILE)*, JPL SIS-FES-014, January 7, 2002.
- [10] *SIRTF Software Interface Specification for IPF Filter Output Files (IFFILE, LGFILE, TARFILE)*, JPL SOS-SIS-2005, November 18, 2002.
- [11] R.J. Brown, *Focal Surface to Object Space Field of View Conversion*. Systems Engineering Report SER No. S20447-OPT-051, Ball Aerospace & Technologies Corp., November 23, 1999.